学位請求論文

および参考論文

森村　浩

学位請求論文

および参考論文

櫟村浩

目次

主論文

The effects of small x resummation on the spin structure function $g_1(x, Q^2)$

公表論文

Does leading ln x resummation predict the rise of g_1 at small x ?

Yuichiro Kiyo, Jiro Kodaira, Hiroshi Tochimura
Zeitschrift für Physik **C74** (1997) 631

参考論文

(1) **On thermal phase structure of deformed Gross-Neveu model**

Haru-Tada Sato, Hiroshi Tochimura
Modern Physics Letters A **11** Nos.39&40 (1996) 3091

(2) **Renormalization of gauge-invariant operators for the structure function $g_2(x, Q^2)$**

Jiro Kodaira, Takashi Nasuno, Hiroshi Tochimura, Kazuhiro Tanaka and Yoshiaki Yasui
Progress of Theoretical Physics **99** No.2 (1998) 掲載決定

(3) **Thermodynamic Gross-Neveu model in a constant electromagnetic field**

Shinya Kanemura, Haru-Tada Sato, Hiroshi Tochimura
Nuclear Physics **B** 掲載決定

主論文

The effects of small x resummation on the spin structure function $g_1(x, Q^2)$

The effects of small x resummation on the spin structure function $g_1(x, Q^2)$

HIROSHI TOCHIMURA
Dept. of Physics, Hiroshima University
Higashi-Hiroshima 739-8526, JAPAN

Abstract

The double logarithmic terms $\alpha_s \ln^2 x$ are important to predict precisely the small x behavior of the spin structure function g_1. We consider the all-order resummation of these logarithmic terms. We numerically analyze the evolution of the flavor non-singlet g_1 structure function taking into account this resummed effect. We include not only the leading logarithmic corrections but also some known next-to-leading logarithmic corrections. It is pointed out that the next-to-leading logarithmic corrections produce an unexpectedly large suppression factor over the experimentally accessible range of x and Q^2. This fact implies that the next-to-leading logarithmic contributions are very important in order to obtain a definite prediction.

Contents

Chapter 1

Introduction

The polarized deep inelastic process is a powerful tool to reveal the internal spin structure of the nucleon. Many experimental and theoretical works have been devoted to this process [1]. Especially, it is important and desirable to get a reliable and precise prediction for the small (Bjorken) x behavior of $g_1(x, Q^2)$ structure function in the light of the Bjorken [2] and Ellis-Jaffe sum rules [3]. Since the verification of these sum rules, which correspond to the fixed (first) moment of g_1 ($\int_0^1 dx g_1(x, Q^2)$), requires the knowledge of the structure function over the entire x region, one has to rely on the theoretical prediction in the experimentally inaccessible small x region.

The small x region corresponds to the Regge limit and we naively expect that the Regge theory may explain the small x behavior of the structure function. Thus, the Regge prediction ($g_1 \sim x^\alpha,\ 0 \leq \alpha \leq 0.5$) [4] has usually been assumed for the extrapolation of the experimental data to the small x region in the old analyses. However, the recent new data [5] show a clear departure of g_1 from the nearly constant behavior of the naive Regge prediction in the small x region. This means that although the Regge theory seems to work well at scales typical for the soft hadron physics, at larger scales, the prediction from this theory becomes unreliable. This fact suggests that the perturbative QCD effects may be very important.

Thanks to the factorization theorem [6], we can apply the perturbative QCD to the

deep inelastic scattering. The factorization theorem guarantees that we can factor out the short-distance part, namely the perturbatively calculable part from the structure function. The structure function is given by the following factorized form

$$g_1(x,Q^2) = \sum_{i=q,\bar{q},g} \int_x^1 C_i(x/y, \alpha_s(\mu^2), Q^2/\mu^2) \Delta f_i(y,\mu^2).$$

where C_i is perturbatively calculable and $\Delta f_i(y,\mu^2)$ is the input (non-perturbative) polarized parton density (x is the Bjorken variable, α_s is the strong coupling constant, Q^2 is the virtuality of the photon and μ^2 is the renormalization scale). If we give an appropriate initial parton density and calculate C_i in perturbation theory, we can predict g_1 over entire x region at scale Q^2. It has been known that there appear two types of logarithmic terms order by order in the perturbative calculation of C_i. One is the single logarithmic (SL) terms $\alpha_s ln Q^2/\mu^2$ and the other is the double logarithmic (DL) terms $\alpha_s \ln^2 x$. The first type logarithmic terms originate from the ultra-violet singularity or the mass singularities and these terms are easily summed to all-orders by Dokshizer-Gribov-Lipatov-Altarelli-Parisi (DGLAP) equation [7] or the renormalization group equation. Recently, various extrapolations of the experimental data to the small x region have been proposed using this DGLAP equation [8] [9] [10]. However, the DL terms seem to give large effects in the small x region and may lead to a drastic change in the the small x prediction from the usual DGLAP prediction. Therefore, if we consider the small x region such that $\alpha_s ln^2 x \sim \mathcal{O}(1)$ we need to re-sum the DL terms to all orders in order to get more reliable predictions (we call this procedure "resummation").

The same problem has already appeared in various QED processes. In the case of QED vertex, we encounter the DL terms $e^2 ln^2 \frac{q^2}{m^2}$ (q is the photon momentum), this logarithmic term gives the large contribution when the absolute value of q^2 is much larger than the external fermion mass m^2. Especially, when $e^2 ln^2 \frac{q^2}{m^2} \sim \mathcal{O}(1)$, the fixed order perturbation theory does not give a good approximation. In order to

extract the correct behavior, we need to sum these logarithmic terms to all-orders. The summation of these terms is considered by Sudakov and it leads to the so-called Sudakov form factor [11]. We also encounter the large logarithmic terms in the case of two body scattering process, *e.g.*, the forward $e^+ + e^- \to \mu^+ + \mu^-$ scattering process. One has the DL terms $e^2 ln^2 \frac{s}{\mu^2}$ (s is the square of the total initial 4-momentum, μ^2 is the arbitrary mass scale). This term again becomes important when $s \to \infty$. The summation was considered in Ref.[12].

For g_1 structure function, Kirschner and Lipatov [13] considered the all order resummation of $\alpha_s \ln^2 x$ series in the case of the virtual photon-quark forward scattering process. Its imaginary part corresponds to the deep inelastic scattering process on the parton target. Recently, Bartels, Ermolaev and Ryskin [14] have given the resummed expression for the partonic g_1^{parton} structure function by using the Infra-Red Evolution Equation and confirmed the results by Kirschner and Lipatov. In addition, they claim that the resummation of double logarithmic terms may lead to larger effects than the usual DGLAP equation. But, when extracting the physical structure function of hadrons from the partonic one, there is possibility that a conclusion at the parton level is not necessarily true. Indeed, the recent numerical analysis by Blümlein and Vogt [15] shows that there are no significant contributions to the evolution of g_1 from the resummation of the leading logarithmic (LL) terms (which are the most dominant terms in the k-th order of perturbation $\sim \alpha_s^k ln^{2k-2} x, k = 1, 2, ..$) in the HERA kinematical region ($x \sim 10^{-3 \sim -5}$).

The different conclusions between at partonic and hadronic level might be coming from the fact that the resummed part of the "coefficient function" (the pertubative part when one chooses $\mu^2 = Q^2$, $C_i(x/y, \alpha_s(Q^2), 1)$) is considered in Ref. [14] but not in Ref. [15]. Blümlein and Vogt did not include the resummed part of the coefficient function because this part turns out to fall in the next-to-leading logarith-

mic (NLL) corrections (which is less singular terms compared with the leading one, $\sim \alpha_s^k ln^{2k-3}x, k = 2, ...$) and depends on the factorization scheme adopted. It is also to be noted that, a slightly steep input density has been used in the analysis of Blümlein and Vogt. The evolution, in general, strongly depends on the input parton densities. The x dependence of $g_1(x, Q^2)$ is given by the convolution of the perturbative part $C_i(x/y, \alpha(\mu^2), Q^2/\mu^2)$ and the input parton densities $\Delta f(y, \mu^2)$ with respect to the longitudinal momentum fraction y. As a result, the x shape of g_1 is determined by both the input parton density and the perturbative part C_i. For example, if we consider a case in which both the input and the perturbative part have a power dependence on x, i.e. $C_i \sim x^{-\alpha}$ and $\Delta f(x) \sim x^{-\lambda}$, we see that the steeper one determines the small x behavior when $x \to 0$. Therefore, if one chooses a steep input function, the perturbative contribution will be completely washed away. One reason for the conclusion by Blümlein and Vogt may be due to this aspect. So it will be interesting to see the sensitivity of the results to the choice of the input densities.

In the present thesis, we analyze the structure function g_1 by taking into account the $\ln x$ resummation. One of the purpose of this thesis is to summarize our present knowledge of the small x resummation physics bearing the future polarized HERA experiment in mind since we do not have data at very small x where the effect of the small x resummation will manifest itself. Thus, we do not make a quantitative test of the validity of the Bjorken sum rules etc.. And in present thesis, we consider the flavor non-singlet part only because we want to clarify the problem of the small x resummation physics by considering the kinematically simple case. It should be straightforward to extend our analysis to the singlet case.

In our analysis, we also take into account the effects of the coefficient function which can not be included consistently at present, since the anomalous dimension has been calculated only at the LL order. The reason is because we could firstly clarify an

origin of different conclusions between the papers by Blümlein and Vogt and Bartels, Ermolaev and Ryskin and secondly get some idea about the magnitude of NLL order corrections in the resummation approach. We consider three different input densities: one is a flat density corresponding to the naive Regge prediction and others are steep ones in the small x region.

This thesis is organized as follows. In chapter 2, the basic knowledge of the deep inelastic lepton nucleon scattering process is summarized. In chapter 3, we make a brief review on the resummation of $\ln x$ series and present an explicit expression for g_1^{NS}. In chapter 4, we show our numerical results and discuss the effects of the NLL corrections . We also give the interpretation of the numerical results. Summary will be given in chapter 5.

Chapter 2

The basic knowledge of deep inelastic scattering

2.1 The kinematics of deep inelastic scattering

We consider the lepton ($l(k)$)- nucleon ($N(p)$) inelastic scattering process,

$$l(k) + N(p) \rightarrow l(k') + X(p_X)$$

where X represents the system of hadrons produced through this process. Experimentally, only the outgoing lepton is detected. The Feynman diagram for this process is depicted in Fig.1 ,where we assume only one photon exchange between the lepton and the nucleon.

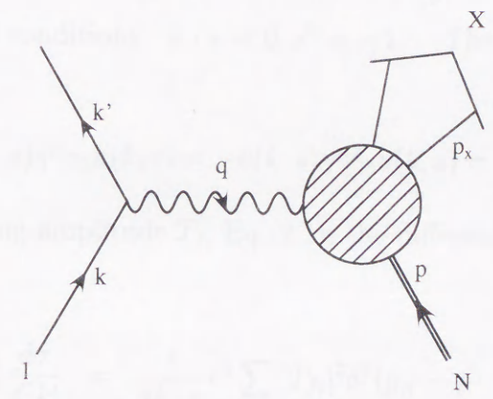

Figure 2.1:

This is a reasonable approximation at present since the average momentum transfer $\langle Q^2 \rangle$ of the experiments is not so large, $\langle Q^2 \rangle \cong 10\ GeV^2$. It is convenient to define the several kinematical variables for this process, the variable $s = (p+k)^2$ corresponds to the total energy squared of the lepton-nucleon system in the center of mass frame, the momentum transfer $Q^2 \equiv -q^2 = -(k-k')^2$, the energy transfer $\nu = p \cdot q/M$ and the Bjorken variable $x \equiv \frac{Q^2}{2p \cdot q}$.

The scattering amplitude is given by,

$$T_{fi} \equiv \langle eX|T|eN\rangle = \bar{u}(k',s')\gamma^\mu u(k,s)\frac{-i}{q^2}\langle X|J^\mu|p,S\rangle \tag{2.1}$$

where s(s') is the polarization vector of the initial(final) lepton, S is the polarization vector of the initial hadron and J^μ is the hadronic electromagnetic current. Here, we mention the spin 4-vector briefly. The spin of fermion is described by a 3-vector $\boldsymbol{s}$ in its rest frame. So we introduce a 4-vector s^μ which reduce to $s^\mu = (0, \boldsymbol{s})$ in the rest frame. Since we normalize 3-vector $\boldsymbol{s}$ as $\boldsymbol{s}^2 = 1$, $s^2 = -1$. The momentum k of the fermion is $k^\mu = (m, \boldsymbol{0})$ in the rest frame, thus, $k \cdot s = 0$. This spin 4-vector s^μ in an arbitrary Lorentz frame is obtained by boosting $s^\mu = (0, \boldsymbol{s})$ from the rest frame. The explicit form of s^μ is,

$$s^\mu = \left(\frac{\boldsymbol{k}\cdot\boldsymbol{s}}{m}, \boldsymbol{s} + \frac{\boldsymbol{k}(\boldsymbol{k}\cdot\boldsymbol{s})}{m(k^0+m)}\right) \tag{2.2}$$

with Lorentz invariant conditions , $k \cdot s = 0, s^2 = -1$. The spin vector is related to the spinors as,

$$\bar{u}(k,s)\gamma^\mu\gamma_5 u(k,s) = -\bar{v}(k,s)\gamma^\mu\gamma_5 v(k,s) = 2ms^\mu$$

By using the scattering amplitude T_{fi} Eq.(2.1), the differential cross section is given by ,

$$\begin{aligned} k'_0\frac{d\sigma}{d^3k'} &= \frac{\pi}{4k\cdot p}e^4\sum_X |T_{fi}|^2\delta^4(p_X - p - q) \\ &= \frac{1}{k\cdot p}\left(\frac{e^2}{4\pi Q^2}\right)^2 L^{\mu\nu}W_{\mu\nu} \end{aligned} \tag{2.3}$$

where e is the charge of the electron. In Eq.(2.3), the leptonic tensor $L^{\mu\nu}$ is defined by

$$\begin{aligned} L^{\mu\nu} &= \frac{1}{2}\sum_{s'} \bar{u}(k,s)\gamma^{\mu}u(k',s')\bar{u}(k',s')\gamma^{\nu}u(k,s) \\ &= k^{\mu}k'^{\nu} + k^{\nu}k'^{\mu} + \frac{q^2}{2}g^{\mu\nu} + im\varepsilon^{\mu\nu\lambda\sigma}q^{\lambda}s^{\sigma} \ . \end{aligned} \tag{2.4}$$

where we used the standard spin projection operator,

$$u(k,s)\bar{u}(k,s) = (\not{k} + m)\frac{1+\gamma_5 \not{s}}{2}$$

Using the Lorentz covariance, current conservation of the QED current, and time reversal and parity invariance, the hadronic tensor $W^{\mu\nu}$ can be parameterized in terms of four structure functions .

$$W_{\mu\nu} \equiv W^{S}_{\mu\nu} + i\, W^{A}_{\mu\nu} \ ,$$

with

$$\begin{aligned} W^{S}_{\mu\nu} &= -\left(g_{\mu\nu} - \frac{q_{\mu}q_{\nu}}{q^2}\right)W_1 + \left(p_{\mu} - \frac{p\cdot q}{q^2}q_{\mu}\right)\left(p_{\nu} - \frac{p\cdot q}{q^2}q_{\nu}\right)\frac{W_2}{M^2} \ , \\ W^{A}_{\mu\nu} &= \varepsilon_{\mu\nu\lambda\sigma}q^{\lambda}\left\{S^{\sigma}MG_1 + (p\cdot qS^{\sigma} - q\cdot Sp^{\sigma})\frac{G_2}{M}\right\} \ . \end{aligned}$$

where M is the mass of the nucleon. These structure functions are related to the dimensionless scaling structure functions as follows,

$$F_1 \equiv W_1 \ , \ F_2 \equiv \frac{\nu}{2M}W_2 \ , \ g_1 \equiv \frac{M\nu}{2}G_1 \ , \ g_2 \equiv \frac{\nu^2}{2}G_2.$$

These are the functions of x and Q^2.

In the target rest frame, the scattering process is conveniently visualized in Fig.(2.2). The kinematical variables in Fig.(2.2) are defined as follows; α is the angle between the spin vector of the target ($\boldsymbol{S}$) and incident electron beam($\boldsymbol{k}$), ϕ is the azimuthal angle between the plane defined by $\boldsymbol{k}$ and $\boldsymbol{k}'$ and θ is the scattering angle. The cross section is calculated from Eq.(2.3) by contracting $L^{\mu\nu}$ with $W^{\mu\nu}$. For the leptonic

tensor $L^{\mu\nu}$, we can use the following approximation, $ms^{\mu} \simeq h_l k^{\mu}$(helicity $h_l = \pm$) because Eq.(2.2) reduces to

$$s^{\mu} = \pm\frac{1}{m}(k\,,\,0\,,\,0\,,\,k^0) \quad , \quad k = |\vec{k}|^2$$

for the longitudinally polarized state, and the lepton mass is negligible, $m_{\text{lepton}} \simeq 0$.

The cross sections can be written as $\sigma^{h_l S} = \overline{\sigma} + h_l \Delta\sigma$ where $\overline{\sigma}$ is the spin independent cross section and $\Delta\sigma$ is the spin dependent cross section.

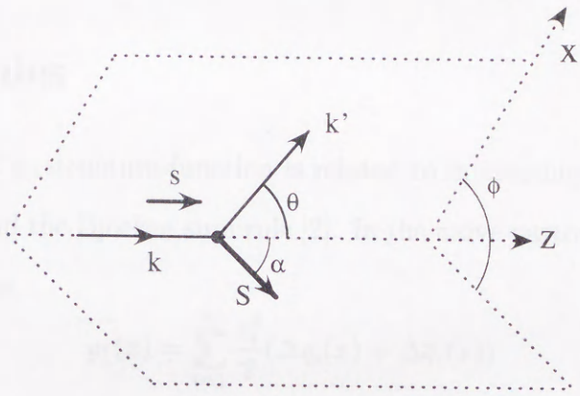

Figure 2.2:

The differential cross section reads

$$\begin{aligned}
&\frac{d\Delta\sigma}{dxdyd\phi} \\
&= \frac{e^4}{4\pi^2 Q^2}\left\{cos\alpha\left\{\left[1-\frac{y}{2}-\frac{y^2}{4}(\kappa-1)\right]g_1(x,Q^2)-\frac{y}{2}(\kappa-1)g_2(x,Q^2)\right\}\right. \\
&- \left. sin\alpha cos\phi\sqrt{(\kappa-1)\left(1-y-\frac{y^2}{4}(\kappa-1)\right)}\left(\frac{y}{2}g_1(x,Q^2)+g_2(x,Q^2)\right)\right\} \qquad (2.5)
\end{aligned}$$

and

$$\frac{d\overline{\sigma}}{dxdyd\phi} = \frac{e^4}{4\pi^2 Q^2}\left\{\frac{y}{2}F_1(x,Q^2)+\frac{1}{2xy}\left(1-y-\frac{y^2}{4}(\kappa-1)\right)F_2(x,Q^2)\right\} \qquad (2.6)$$

where $y = Q^2/sx$ and $\kappa - 1 \equiv M^2Q^2/\nu^2 = 4M^2x^2/Q^2$. We obtain the longitudinal asymmetry which is the difference between the cross section for the nucleon's spin being

parallel to the lepton's ($\uparrow\uparrow$) and the nucleon's spin being anti-parallel to the lepton's ($\uparrow\downarrow$) :

$$\frac{d\sigma^{\uparrow\uparrow}}{dxdy} - \frac{d\sigma^{\uparrow\downarrow}}{dxdy} = \frac{e^4}{\pi Q^2}\left\{\left[1 - \frac{y}{2} - \frac{y^2}{4}(\kappa - 1)\right] g_1(x, Q^2) - \frac{y}{2}(\kappa - 1) g_2(x, Q^2)\right\}$$

where the azimuthal angle ϕ has been integrated out, since the longitudinal asymmetry is independent of ϕ. Notice that $g_2(x, Q^2)$ comes in with a factor $\kappa - 1 = \frac{(2Mx)^2}{Q^2}$. So when Q^2 is large, we can neglect $g_2(x, Q^2)$ in this expression. Thus, the longitudinal asymmetry can be used to measure the structure function $g_1(x, Q^2)$.

2.2 Sum rules

The first moment of g_1 structure function is related to interesting sum rules, the Ellis-Jaffe sum rule [3], and the Bjorken sum rule [2]. In the naive parton model, g_1 structure function is written as,

$$g_1(x) = \sum_{i=1}^{n_f} \frac{e_i^2}{2}(\Delta q_i(x) + \Delta\overline{q}_i(x)) \tag{2.7}$$

where $\Delta q_i = q_i^+ - q_i^-$ ($\Delta\overline{q}_i = \overline{q}_i^+ - \overline{q}_i^-$) is the polarized parton (anti-parton) density, the difference of parton densities whose spins are parallel and anti-parallel to the nucleon's spin. e_i is the electric charge of the quark (flavor i) and n_f is the number of quark flavors involved. The first moment of g_1 becomes for three flavors from Eq.(2.7),

$$\Gamma_1^p = \int_0^1 dx g_1^p = \frac{1}{2}(\frac{4}{9}(\Delta u + \Delta\overline{u}) + \frac{1}{9}(\Delta d + \Delta\overline{d}) + \frac{1}{9}(\Delta s + \Delta\overline{s})) \tag{2.8}$$

and , from isospin invariance,

$$\Gamma_1^n \equiv \int_0^1 g_1^n(x) = \frac{1}{2}(\frac{4}{9}(\Delta d + \Delta\overline{d}) + \frac{1}{9}(\Delta u + \Delta\overline{u}) + \frac{1}{9}(\Delta s + \Delta\overline{s})) \tag{2.9}$$

where $\Delta q \equiv \int_0^1 dx \Delta q(x)$, $\Delta\overline{q} \equiv \int_0^1 dx \Delta\overline{q}(x)$ are the first moment of the polarized parton densities in the proton. By taking the appropriate combinations of the first moment Δq_i, we can rewrite Eqs.(2.8,2.9) as

$$\Gamma_1^{p(n)} = \frac{1}{12}\left[+(-)a_3 + \frac{1}{3}a_8\right] + \frac{1}{9}\Delta\Sigma \tag{2.10}$$

where

$$\begin{aligned}
\Delta\Sigma &= \Delta u + \Delta\overline{u} + \Delta d + \Delta\overline{d} + \Delta s + \Delta\overline{s} \\
a_3 &= \Delta u + \Delta\overline{u} - (\Delta d + \Delta\overline{d}) \\
a_8 &= \Delta u + \Delta\overline{u} + \Delta d + \Delta\overline{d} - 2(\Delta s + \Delta\overline{s}).
\end{aligned}$$

The combination a_3 is related to the neutron β-decay constant $|g_A/g_V|$. Under the $SU(3)$ flavor symmetry, a_3 and a_8 are related to the symmetric and anti-symmetric weak $SU(3)_f$ couplings F and D,

$$\begin{aligned}
a_3 &= \left|\frac{g_A}{g_V}\right| = F + D \\
a_8 &= 3F - D
\end{aligned}$$

There is no theoretical prediction for $\Delta\Sigma$. However, if we assume that the strange sea in the nucleon is unpolarized $\Delta s = 0$, $a_8 = \Delta\Sigma$ and Eq.(2.10) leads to the Ellis-Jaffe sum rule,

$$\Gamma_1^{p(n)} = +(-)\frac{1}{12}(F + D) + \frac{5}{36}(3F - D). \tag{2.11}$$

The violation of this prediction for the proton found by the EMC [16] is one reason of the revived interests in the polarized deep inelastic scattering.

The Bjorken sum rule is obtained from Eq.(2.10) as,

$$\Gamma_1^p - \Gamma_1^n = \frac{1}{6}\left|\frac{g_A}{g_V}\right|. \tag{2.12}$$

This sum rule was derived by Bjorken from the light cone current algebra and isospin invariance.

Now the above sum rules should be receive QCD corrections. Therefore it is interesting and important to see how the QCD corrections modify the above sum rules. There are two issues when one tackles this problem. The first is the QCD corrections to the right-hand side of Eq.(2.10). For example, this corrections to the Bjorken sum

rule, now is calculated up to $o(\alpha_s^3)$ [17] [18].

$$\Gamma_1^p - \Gamma_1^n = \frac{1}{6}\left|\frac{g_A}{g_V}\right|\left[1 - \frac{\alpha_s}{\pi} - 3.58\left(\frac{\alpha_s}{\pi}\right)^2 - 20.2\left(\frac{\alpha_s}{\pi}\right)^3 + \cdots\right]. \tag{2.13}$$

The second issue is how to obtain the moment from the experimental data which have information on only restricted values of x. In order to settle these problems, it is inevitable to study the QCD effects on g_1 structure function itself. In the next chapter, we consider the QCD effects on the g_1 structure function.

Chapter 3

The resummation of logarithmic terms

3.1 The necessity of the resummation

The flavor non-singlet part of the polarized structure function g_1^{NS} is given by the formula,

$$g_1^{NS}(Q^2,x) = \frac{\langle e^2\rangle}{2}\int_x^1 \frac{dy}{y} C^{NS}(\alpha_s(Q^2), x/y)\Delta q^{NS}(Q^2,y)\ , \tag{3.1}$$

where Δq^{NS} is the flavor non-singlet combination of the polarized parton densities,

$$\Delta q^{NS}(Q^2,x) = \sum_{i=1}^{n_f} \frac{e_i^2 - \langle e^2\rangle}{\langle e^2\rangle}(\Delta q_i(Q^2,x) + \Delta\overline{q}_i(Q^2,x))\ ,$$

and C^{NS} is the coefficient function. n_f is the number of active flavors with electric charge e_i, $\langle e^2\rangle = \sum e_i^2/n_f$. The perturbative evolution of the parton density is controlled by the DGLAP equation,

$$Q^2\frac{\partial}{\partial Q^2}\Delta q(Q^2,x) = \int_x^1 \frac{dy}{y} P(\alpha_s(Q^2), x/y)\Delta q(Q^2,y)\ . \tag{3.2}$$

In the above equation and in the following, we suppress the superscript *NS* which means the flavor non-singlet part. The coefficient function $C(\alpha_s, y)$ and the splitting function $P(\alpha_s, y)$ are both calculable in the QCD perturbation theory. When x is finite, it may be enough to compute them to the fixed-order of perturbation. In the small x region, however, the fixed-order calculation becomes questionable since there appear

$\ln^n x$ corrections in the higher orders of the strong coupling constant α_s. If these $\ln^n x$ terms compensate the smallness of α_s, we must resum the perturbative series to the all orders to get a reliable prediction.

To see what terms show up at small x, it will be convenient to take the Mellin transform of Eq.(3.1).

$$\begin{aligned} g_1(Q^2, N) &\equiv \int_0^1 dx x^{N-1} g_1(Q^2, x) \\ &= \frac{\langle e^2 \rangle}{2} C(\alpha_s(Q^2), N) \Delta q(Q^2, N) \ , \end{aligned} \tag{3.3}$$

where

$$\begin{aligned} C(\alpha_s(Q^2), N) &\equiv \int_0^1 x^{N-1} C(\alpha_s(Q^2), x) \ , \\ \Delta q(Q^2, N) &\equiv \int_0^1 x^{N-1} \Delta q(Q^2, x) \ . \end{aligned}$$

The DGLAP evolution equation Eq.(3.2) becomes,

$$Q^2 \frac{\partial}{\partial Q^2} \Delta q(Q^2, N) = -\gamma(\alpha_s(Q^2), N) \Delta q(Q^2, N) \ . \tag{3.4}$$

Here the anomalous dimension γ is the moment of the splitting function,

$$\gamma(N, \alpha_s(Q^2)) \equiv -\int_0^1 dx x^{N-1} P(\alpha_s(Q^2), x) \ .$$

Eq.(3.4) is easily solved to give,

$$\Delta q(Q^2, N) = \Delta q(Q_0^2, N) \exp\left(-\int_{\alpha_s(Q_0^2)}^{\alpha_s(Q^2)} \frac{d\alpha}{\beta(\alpha)} \gamma(\alpha, N) \right) \ ,$$

where β is the beta function,

$$\beta(\alpha_s) = \frac{\partial \alpha_s}{\partial \ln Q^2} = \alpha_s \left[-\beta_0 \frac{\alpha_s}{4\pi} - \beta_1 (\frac{\alpha_s}{4\pi})^2 - \cdots \right] \ .$$

The first two coefficients of the β function are,

$$\beta_0 = \frac{11}{3} C_A - \frac{4}{3} T_R n_f \quad , \quad \beta_1 = \frac{34}{3} C_A^2 - \frac{20}{3} C_A T_R n_f - 4 C_F T_R n_f \ ,$$

with $C_F = (N_c^2 - 1)/2N_c$ and $C_A = N_c$ for the SU(N_c) color group and $T_R = 1/2$.

The coefficient function $C(\alpha_s, N)$ and the anomalous dimension $\gamma(\alpha_s, N)$ may be expanded in the powers of α_s,

$$\begin{aligned} C(\alpha_s, N) &= 1 + \sum_{k=1}^{\infty} c^k(N) \bar{\alpha}_s^k \ , \\ \gamma(\alpha_s, N) &= \sum_{k=1}^{\infty} \gamma^k(N) \bar{\alpha}_s^k \ . \end{aligned}$$

where (and in the following) we use the abbreviation,

$$\bar{\alpha}_s \equiv \frac{\alpha_s}{4\pi} \ .$$

The singular behaviors of the coefficient and splitting functions as $x \to 0$ appear as the pole singularities at $N = 0$ in the moment space since the singularities in N^{-m} correspond to the $\ln^{m-1}\left(\frac{1}{x}\right)$ singularities. The explicit next-to-leading order (NLO) calculations of the coefficient function [18] and the anomalous dimension [19] in the $\overline{\rm MS}$ scheme show a strong singularity at $N = 0$,

$$\begin{aligned} c^1(N) &= 2C_F \frac{1}{N^2} + \mathcal{O}\left(\frac{1}{N}\right) \ , \\ \gamma^2(N) &= 4(3C_F^2 - 2C_A C_F) \frac{1}{N^3} + \mathcal{O}\left(\frac{1}{N^2}\right) \ , \end{aligned} \tag{3.5}$$

whereas the leading order anomalous dimension looks like,

$$\gamma^1(N) = -2C_F \frac{1}{N} - C_F + \mathcal{O}(N) \ ,$$

at small N. These strong singularities (double logarithmic corrections) will persist to all orders of perturbative series. Indeed, at the k-th loop, the anomalous dimension and the coefficient function are expected to behave as,

$$\gamma^k(N) \sim N \left(\frac{1}{N^2}\right)^k \quad , \quad c^k(N) \sim \left(\frac{1}{N^2}\right)^k \ . \tag{3.6}$$

Our task is to resum these terms to all-orders in the perturbative expansion. In the next section, we will explain how to resum these leading singular terms to all-orders

of the perturbative expansion. Before discussing the details of the resummation procedure, it may be worth mentioning the difference between the polarized (unpolarized flavor non-singlet) and the unpolarized flavor singlet structure functions [20]. Naively one expects for the unpolarized structure function that the anomalous dimension behaves like $\gamma \sim \alpha_s^k/N^{2k-1}$ at the k-th loop* because there exist extra infra-red and collinear singularities. In the case of the unpolarized flavor singlet structure functions, however, many of them are canceled and the true behavior at the k-th loop is $\gamma \sim (\alpha_s/N)^k$. These terms can be resummed by the Balitskii-Fadin-Kuraev-Lipatov (BFKL) [21] equation. On the other hand, above strong singularities survive in the polarized structure function. This fact suggests that the polarized structure function will receive large perturbative corrections at small x.

3.2 The double logarithmic approximation (DLA) for flavor non-singlet g_1 structure function

Consider the virtual photon (mass Q^2) quark forward scattering process whose imaginary part corresponds to the structure function of parton. Let us explain which term is important in various kinematical region in perturbation theory. For this purpose, it is important to note that, in the perturbative calculation, we obtain, in general, the following types of logarithms order by order in α_s expansion

$$(\alpha_s ln Q^2/\mu^2)^n, \qquad (\alpha_s ln^2 x)^n, \qquad (\alpha_s ln x ln Q^2/\mu^2)^n. \tag{3.7}$$

μ^2 is the virtuality of the initial parton. Firstly consider the kinematical region, $x \sim \mathcal{O}(1)$ and large Q^2. In this case, the only large logarithm is lnQ^2/μ^2, since $lnx \simeq \mathcal{O}(1)$. Therefore to get a reliable prediction, we must sum up these large logarithms $(lnQ^2/\mu^2)^n$ to all orders. And the result of this summation coincide with the results of DGLAP evolution equation. The Feynman diagram of the ladder type (Fig.3.1)

*We follow the convention of Ref. [34].

corresponds to this summation. These terms come from the kinematical region where the transverse momenta k_{jT} of virtual partons (quarks and gluons) are strongly ordered,

$$\mu^2 \ll \cdots \ll k_{2T}^2 \ll k_{1T}^2 \ll Q^2. \tag{3.8}$$

Indeed, the Leading Order (LO) DGLAP result has been reproduced by calculating this ladder diagram under the strong ordering Eq.(3.8) [22] [23].

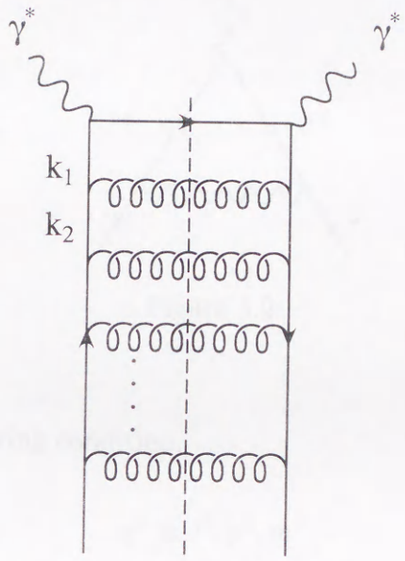

Figure 3.1:

On the other hand, in the small x region, the most important terms are double logarithmic (DL) terms, $(\alpha_s ln^2 x)^n$ and $(\alpha_s lnx lnQ^2/\mu^2)^n$. Then, in this kinematical region we must sum these terms to all-orders as already explained in the previous section, and this will give a reliable approximation. We call this approximation the double logarithmic approximation (DLA). As well known([12], we will see later), the ordering Eq.(3.8) is not valid for evaluating the leading double logarithmic terms in this kinematical region. Furthermore, one must consider not only the ladder type Feynman diagrams but also non-ladder type Feynman diagrams. Before going to the

somewhat complicated QCD case, let us go back to the QED process which gives the same logarithmic terms [24].

Consider the one-loop diagram for the QED vertex Fig.3.2. The analytical form is

$$\Gamma^1_\mu(p,l,q^2) = -ie^2 \int \frac{d^4k}{(2\pi)^4} \frac{\gamma_\nu(\not{l}-\not{k}+m)\gamma_\mu(\not{p}-\not{k}+m)\gamma^\nu}{[(l-k)^2-m^2+i\varepsilon][(p-k)^2-m^2+i\varepsilon][k^2+i\varepsilon]}. \tag{3.9}$$

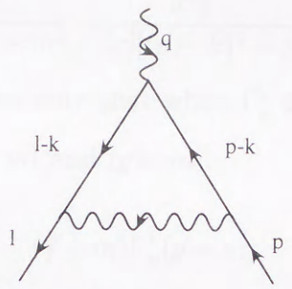

Figure 3.2:

Now, we assume the following condition,

$$q^2 \gg l^2, p^2, m^2. \tag{3.10}$$

This condition means,

$$|p\cdot l| \sim \frac{1}{2}|q^2| \gg l^2, p^2, m^2 \tag{3.11}$$

In the following calculation, we will use the Sudakov decomposition [11] for the loop momenta k,

$$k = \alpha l + \beta p + k_T \tag{3.12}$$

where k_T is the transverse component of the vector k orthogonal to the vectors p and l, $k_T \cdot p = k_T \cdot l = 0$. The DL term comes from the region in which the internal photon momentum becomes soft, namely,

$$k = \alpha l + \beta p + k_T \sim 0.$$

This means that

$$|\alpha|, |\beta| \ll 1, \quad k_T \sim 0. \tag{3.13}$$

Then, we can neglect k in the numerator of the integrand. Γ^1_μ becomes,

$$\Gamma^1_\mu(p, l, q^2) = -i\frac{e^2}{(2\pi)^4}\gamma_\nu(\not{l} + m)\gamma_\mu(\not{p} + m)\gamma^\nu I_1 \tag{3.14}$$

where,

$$I_1 = \int \frac{d^4k}{[(l-k)^2 - m^2 + i\varepsilon][(p-k)^2 - m^2 + i\varepsilon][k^2 + i\varepsilon]}. \tag{3.15}$$

Eq.(3.14) can be simplified, if we note that when Γ^1_μ appears in diagrams it is always multiplied by the matrices $(\not{l} + m)$ and $(\not{p} + m)$:

$$(\not{l} + m)\Gamma^1_\mu(\not{p} + m) \tag{3.16}$$

By using the condition Eq.(3.11), we obtain,

$$(\not{l} + m)\Gamma^1_\mu(\not{p} + m) \sim -i\frac{e^2}{(2\pi)^4}4p \cdot l(\not{l} + m)\gamma_\mu(\not{p} + m)I_1, \tag{3.17}$$

thus,

$$\Gamma^1_\mu = i\frac{e^2}{(2\pi)^4}2t\gamma_\mu I_1 \tag{3.18}$$

where

$$t = q^2 \sim -2(p \cdot l) \tag{3.19}$$

Next, we consider the calculation of I_1. From the conditions Eq.(3.13), we can approximate the denominator,

$$k^2 = (\alpha p + \beta l)^2 + k_T^2 \sim -t\alpha\beta - \rho \tag{3.20}$$

$$|\alpha t|, |\beta t| \gg \rho \gg \mu^2 \tag{3.21}$$

($\rho \equiv -k_T^2 > 0$ since k_T is space-like 4-vector)

$$(l-k)^2 = ((1-\alpha)l - \beta p - k_T)^2 \sim -\beta t \tag{3.22}$$

$$(p-k)^2 = (-\alpha l + (1-\beta)p - k_T) \sim -\alpha t \tag{3.23}$$

Then,

$$I_1 = -\frac{\pi}{2|t|}\int \frac{d\rho}{\rho + t\alpha\beta - i\varepsilon}\frac{d\alpha}{\alpha}\frac{d\beta}{\beta} \tag{3.24}$$

where we used the relation, $d^4k \sim \frac{1}{2}\pi|t|d\alpha d\beta$. In accordance with the condition Eq.(3.21), we carry out the integration with respect to ρ,

$$\int_0^{min[|t\alpha|,|t\beta|]} \frac{d\rho}{\rho + t\alpha\beta - i\varepsilon} = logmin\left\{\frac{1}{|\alpha|},\frac{1}{|\beta|}\right\} + \frac{i\pi}{2}[1 - sign(t\alpha\beta)] \tag{3.25}$$

Since the first term vanishes after integration with respect to α or β, only the second term survives. The integral regions for the α and β are given by the conditions of Eqs.(3.22,3.23) ($\alpha\beta t < 0 \quad p^2/q^2 < |\alpha| < 1, \quad l^2/q^2 < |\beta| < 1$) Finally, we obtain the double logarithmic term,

$$\Gamma^1_\mu = -\frac{\alpha_{QED}}{8\pi^2}\gamma_\mu ln\frac{q^2}{l^2}ln\frac{q^2}{p^2}.$$

In the kinematical region when $q^2 \to \infty$, this logarithmic term gives large contribution and the fixed order perturbation is not applicable. In order to get a correct asymptotic behavior, we must consider the sum of these DL terms over the entire perturbation series. Sudakov considered the summation of the DL terms for the QED vertex and obtained the so-called Sudakov form factor;

$$\Gamma^{Sudakov}_\mu = \gamma_\mu exp\left\{-\frac{\alpha_{QED}}{8\pi^2}ln\frac{q^2}{l^2}ln\frac{q^2}{p^2}\right\} \tag{3.26}$$

Next example is the $e^+e^- \to \mu^+\mu^-$ forward scattering process. The DL terms come from the region in which the internal fermions and photons become soft. This fact may be understood easily from the explicit calculation of a lower order diagram. Within the one-loop corrections for this process, Figs.3.3 and Fig.3.4 give the DL contribution.

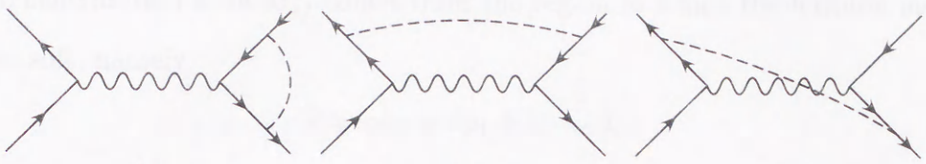

Figure 3.3:

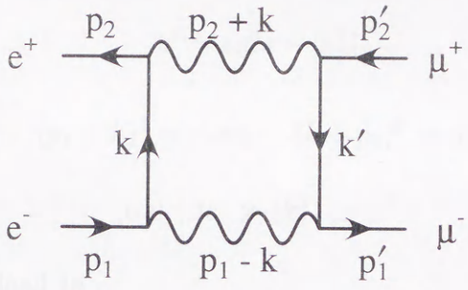

Figure 3.4:

Firstly, consider Figs.3.3. It is easily understood that the DL term comes from the region in which the virtual photon momentum becomes soft. (The dashed line in Figs.3.3 represents the soft photon.) Indeed, Fig.3.3a gives the DL term e^2ln^2s/μ^2 since this diagram includes Γ^1_μ we have calculated already. Calculating the diagram taking into account the virtual photon being soft, we obtain the DL term

$$e^2ln\ |u|/\mu^2 \sim e^2ln\ s/\mu^2 \tag{3.27}$$

(μ^2 is the arbitrary mass scale) for Fig.3.3c and

$$e^2ln\ t/\mu^2 \tag{3.28}$$

for Fig.3.3b. Now, since $t \sim \mu^2$, Fig.3.3b does not contribute. Figs.3.3a,c contribute when $s \to \infty$. The amplitude M^1_{sf} for Fig.3.4 is given by,

$$M^1_{sf} = e^4 \int \frac{d^4k}{(2\pi)^4} \frac{\bar{u}(p_1)\gamma^\mu \not{k}\gamma^\nu v(p_2)\bar{v}(p_2)\gamma_\nu \not{k}\gamma_\mu u(p_1)}{(k^2+i\varepsilon)^2[(p_1-k)^2+i\varepsilon][(p_2+k)^2+i\varepsilon]} \tag{3.29}$$

The DL contribution from M^1_{sf} comes from the region in which the fermion momenta becomes soft, namely,

$$k = \alpha p_2 + \beta p_1 + k_T \sim 0,$$

This means that

$$|\alpha|, |\beta| \ll 1, \quad k_T \sim 0. \tag{3.30}$$

Therefore, we can use the following approximation for the denominator of Eq.(3.29),

$$k^2 = \alpha\beta s - |k_T^2| \tag{3.31}$$

$$(p_1 - k)^2 \simeq -\alpha s, \quad (k + p_2)^2 \simeq \beta s \tag{3.32}$$

$$|\alpha s|, |\beta s| \gg |k_T^2| \gg \mu^2 \tag{3.33}$$

These approximations lead to ,

$$M^1_{sf} = -e^4 \int \frac{d^4k}{(2\pi)^4} \frac{\bar{u}(p_1)\gamma^\mu \not{k}\gamma^\nu v(p_2)\bar{v}(p_2)\gamma_\nu \not{k}\gamma_\mu u(p_1)}{(\alpha\beta s - |k_T^2| + i\varepsilon)^2\alpha\beta}. \tag{3.34}$$

Taking into account the fermion being soft $k \sim 0$, the numerator is simplified as [12],

$$\begin{aligned} \bar{u}(p_1)\gamma^\mu \not{k}\gamma^\nu v(p_2)\bar{v}(p_2)\gamma_\nu \not{k}\gamma_\mu u(p_1) &\sim -1/2k_T^2 \bar{u}(p_1)\gamma^\mu\gamma_\sigma\gamma^\nu v(p_2)\bar{v}(p_2)\gamma_\nu\gamma_\sigma\gamma_\mu u(p_1) \\ &= -2k_T^2 \bar{u}(p_1)\gamma^\mu v(p_2)\bar{v}(p_2)\gamma_\mu u(p_1). \end{aligned} \tag{3.35}$$

Therefore, we can extract the Born spin structure from the 1 loop box amplitude,

$$M^1_{sf} = M^0_{sf} J^1.$$

where,

$$M^0_{sf} = ie^2 \frac{\bar{u}(p_1)\gamma_\mu v(p_2)\bar{v}(p_2)\gamma^\mu u(p_1)}{s}. \tag{3.36}$$

The amplitude J^1 becomes,

$$J^1 \sim -\frac{ie^2}{16\pi^3} \int \frac{d\alpha d\beta d|k_T^2||k_T^2|}{(\alpha\beta s - |k_T^2| + i\varepsilon)^2\alpha\beta}$$

where we change the measure, $d^4k = \pi\frac{s}{2}d\alpha d\beta d|k_T^2|$. We use the relation for the numerator,

$$|k_T^2| = -(\alpha\beta s - |k_T^2|) + \alpha\beta s$$

and neglect the second term because this part cancels simple poles α and β which lead to the logarithmic contribution.

Then , we get

$$J^1 \sim -\frac{ie^2}{16\pi^3}\int \frac{d\alpha d\beta d|k_T^2|}{\alpha\beta(|k_T^2| - \alpha\beta s - i\varepsilon)}$$

In accordance with the condition Eq.(3.33), the integration over $d|k_T^2|$ is taken from 0 to the smaller one among $|\alpha s|$ and $|\beta s|$; the result is

$$\int_0^{min(|\alpha s|,|\beta s|)} \frac{d|k_T^2|}{(|k_T^2| - \alpha\beta s + i\varepsilon)} = ln\ min\left[\frac{1}{|\alpha|}, \frac{1}{|\beta|}\right] + \frac{i\pi}{2}[1 + sign(s\alpha\beta)]$$

Since the first term vanishes after integration with respect to α or β, only the second term survives. The integral regions for α and β are given by the conditions of Eqs.(3.32) $(\alpha\beta s > 0 \quad \frac{\mu^2}{s} < |\alpha| < 1, \quad \frac{\mu^2}{s} < |\beta| < 1)$

Finally we obtain the double logarithmic result,

$$\begin{aligned} J^1 &= \frac{e^2}{16\pi^2}\int \frac{d\alpha d\beta}{\alpha\beta} \\ &= \frac{e^2}{16\pi^2}\left(\int_{\mu^2/s}^1 \frac{d\alpha}{\alpha}\int_{\mu^2/s}^1 \frac{d\beta}{\beta} + \int_{-1}^{-\mu^2/s} \frac{d\alpha}{\alpha}\int_{-1}^{-\mu^2/s} \frac{d\beta}{\beta}\right) \\ &= \frac{e^2}{8\pi^2} ln^2 \frac{s}{\mu^2}. \end{aligned}$$

The summation of these double logarithmic terms has been performed firstly in Ref.[12] for the $e^+e^- \to \mu^+\mu^-$ forward scattering process utilizing the Bethe-Salpeter equations.

Now, we proceed to the summation of the DL terms for the photon-quark scattering process[13], Firstly, consider the DL approximation (DLA) of the quark-antiquark forward scattering amplitude $A(s,t)$, because this amplitude is a part of the photon-quark

scattering. Using the fact that the spin structure of the Born amplitude is maintained in the higher orders in the DLA (see the previous box diagram calculation and Ref.[12]), we factor out the Born amplitude,

$$A(s,t) = b_0(s,t)M(s,t)$$

where b_0 is the Born amplitude and we include g^2 (g is the QCD coupling constant) into the definition $M(s,t)$. Before going to calculations of the amplitude, let us decompose the amplitude into parts with definite quantum numbers of the gauge group SU(N_c) in the exchange channel. Generally, in SU(N_c), the amplitude can be decomposed into a singlet(0)state and a vector state(V)

$$M_{ab}^{a'b'} = P_{0ab}^{a'b'} M_0 + P_{Vab}^{a'b'} M_V \tag{3.37}$$

a,b and a', b' label the color states of the initial and final quarks. The projectors $P_{0ab}^{a'b'}$ and $P_{Vab}^{a'b'}$ are given respectively as

$$P_{0ab}^{a'b'} = \frac{1}{N_c}\delta_{aa'}\delta_{bb'}, \tag{3.38}$$

$$P_{Vab}^{a'b'} = \delta_{ab}\delta_{a'b'} - \frac{1}{N_c}\delta_{aa'}\delta_{bb'} \tag{3.39}$$

In Born level, M_0 and M_V are,

$$M_0^{Born} = \frac{N_c^2 - 1}{2N_c}g^2, \qquad M_V^{Born} = -\frac{1}{2N_c}g^2. \tag{3.40}$$

For the later convenience, we consider color structure for the diagrams Figs.3.6. The color component of the blob can be written as vector,

$$M = (M_0, M_V)$$

Then, the change of the color structure due to the additional gluon is given by multiplying the amplitude by a certain matrix, $\hat{m} \cdot M$. The matrices have different element for

the graphs of Fig.3.6a (s-channel gluon) ,Fig.3.6b(t-channel gluon) Fig.3.6c(u-channel gluon)

$$\hat{m}_s = \begin{pmatrix} 0 & \frac{N_c^2-1}{2N_c} \\ \frac{1}{2N_c} & \frac{N_c^2-2}{2N_c} \end{pmatrix}, \quad \hat{m}_u = \begin{pmatrix} 0 & \frac{N_c^2-1}{2N_c} \\ \frac{1}{2N_c} & -\frac{1}{N_c} \end{pmatrix}$$

$$\hat{m}_s - \hat{m}_u + \hat{m}_t = \frac{N_c^2 - 1}{2N_c} I$$

where I is the 2×2 unit matrix.

Now, we proceed to the calculations of the amplitude. It is not difficult to apply the method developed in QED calculation [12] to QCD. Indeed, at one-loop level the calculation will be almost the same. However, we need to calculate more complicated higher order diagrams and it has been well-known that the application of this method to the negative signature amplitude (see,Eq.(3.43)) which is relevant to the polarized photon quark scattering is much more complicated [27]. Then, the more easier method has been developed in Ref.[13]. Generally, the infra-red singularities appear in the perturbative calculation if one consider the theory which include the mass-less particle. It is well-known that all infra-red singularities cancel by considering the inclusive process due to the Bloch-Nordsieck theorem and KLN (Kinoshita-Lee-Nauenberg) theorem. Thus, QED processes are free from infra-red singularities. However, in the process which include hadrons in the initial state e.g. deep inelastic scattering, one cannot get rid of the mass singularity arising from the initial state. This problem is avoided by the factorization theorem. According to this theorem, the mass singularity factors out and it is absorbed into the non-perturbative part. Namely, for the perturbative calculation of the forward virtual photon quark scattering, we obtain the cross section, schematically writing,

$$\sigma = 1 + ag^2 ln(Q^2/m^2) + \cdots \tag{3.41}$$

where m^2 is a quark mass. The second term becomes singular when $m^2 \to 0$. The

factorization theorem guarantees that the cross section becomes the following form in which the mass singularity is factorized,

$$\sigma = (1 + ag^2 ln(Q^2/\mu^2) + \cdots)(1 + ag^2 ln(\mu^2/m^2) + \cdots). \tag{3.42}$$

The part including m^2 is absorbed into the distribution function. Anyway, we need to regulate the infra-red singularities by introducing the infra-red cut off μ in the calculation of quark scattering process. Since the QCD coupling constant is written at the leading order as,

$$g^2(\mu^2) = \frac{1}{\beta_0 ln\ Q^2/\Lambda^2_{QCD}}$$

we choose the value of μ as much greater than Λ_{QCD} so that perturbative calculations are still applicable,

$$g^2(\mu^2) \ll 1.$$

We have shown by explicit calculation of the QED process that the DL term comes from the region in which the internal fermion and gauge particles become soft . This means that the momentum of this soft fermion can reach the infra-red cut off μ^2. The idea of Ref.[13] is the generalization of this 1-loop discussion ,namely, their procedure consists in isolating the softest virtual particle in the general diagrams. There are some good aspects in this procedure. It turns out that ,after isolating the softest particle, the remaining particles can be put on the mass-shell. Therefore,it is not necessary to consider the off-mass-shell amplitudes and to analyze complicated higher order graphs. Moreover, we simply deal with gauge invariant set of graphs, because only the on-mass shell amplitudes appear in this approach. On the other hand, one shortcoming is the following. In this approach, all singularities are regularized by one scale μ^2, so the factorization of mass singularities becomes implicit and ambiguous. We will come back to this point in the next section. We use the Feynman gauge in the following calculation. According to this method, we isolate the softest particle in

graphs. Firstly, let us consider the case that the softest particle is a quark. In this case, the diagram involving the two quark lines in the crossed channel Fig.3.5 gives the DL contribution. The double logarithmic contribution arise from the region in which the loop momenta of these two quark lines become smaller than the remaining loop momenta.

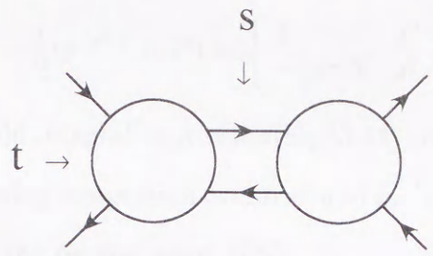

Figure 3.5:

This fact may be understood easily by returning to the QED process calculation, because Fig.3.5 just reduces to Fig.3.4 at one loop order. Notice that we can regard the blobs of Fig.3.5 as the on-mass shell amplitude with the cut-off k_T^2, since the internal quark lines are nearly on the mass shell in the DL approximation.

The amplitude of Fig.3.5 is given by

$$M_i^p(s,\mu^2)|_{quark} = \frac{-i}{(2\pi)^4}\int \frac{s^2 d\alpha d\beta d^2k_T(-2k_T^2)}{2(k_T^2+\alpha\beta s+i\varepsilon)^2}\frac{M_i^p(s\alpha,|k_T^2|)}{s\alpha+i\varepsilon}\frac{M_i^{p'}(-s\beta,|k_T^2|)}{-s\beta+i\varepsilon}$$

where the soft quark approximation Eqs.(3.32) was used and the suffix i represent the color state. It is convenient to expand M into the partial waves $f(N)$. The variable N corresponds to the angular momentum in the complex plane. In order to express the amplitude in terms of partial waves and analytically continue to the complex N plane, one must divide it into symmetric and antisymmetric parts with respect to the transformation $s \leftrightarrow u \simeq -s$,

$$M^{\pm} = \frac{1}{2}[M(s) \pm M(-s)] \tag{3.43}$$

The even (odd) part of the amplitude is related to the positive (negative) signature partial wave via the Sommerfeld-Watson transformation,

$$M^p(s,\mu^2) = \int_{\delta-i\infty}^{\delta+i\infty} \frac{dN}{2\pi i} \xi^p(N) f^p(N) (\frac{s}{\mu^2})^N \tag{3.44}$$

where δ is chosen so that the integration contour in Eq.(3.44) is on the right of the singularities of $f^p(N)$. The signature factor ξ^p is given by

$$\xi^p(N) = \frac{1}{2}(e^{-i\pi N} + P) \approx \begin{cases} 1 & P = +1 \\ -\frac{1}{2} i\pi N & P = -1 \end{cases}$$

Substituting the Sommerfeld integral expression(Eq.(3.44)) into the double logarithmic amplitudes M, and performing integration over α, β and k_T [13], we obtain the following soft quark contribution to the partial wave $f(N)$

$$f_i^p(N)|_{quarks} = \frac{1}{8\pi^2} \frac{1}{N} (f_i^p(N))^2. \tag{3.45}$$

Until now, we have considered only the diagrams in which the softest particle is a quark. However, the DL contributions is not exhausted by soft-quarks. Next consider the case that the softest virtual particle is a gluon, Figs.3.6.

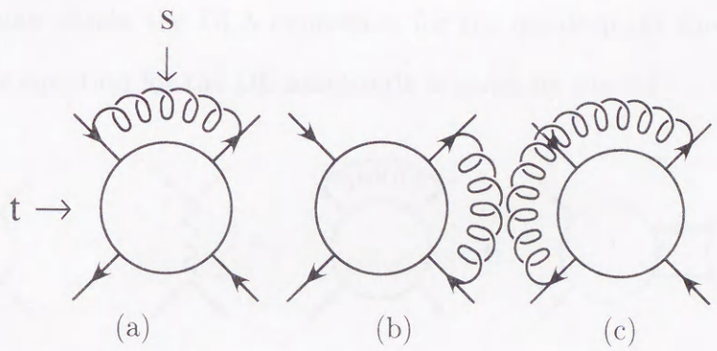

Figure 3.6:

It is not difficult to see that these diagrams contribute to the DLA based on the same argument for the soft quark case. In the forward scattering process, the s-channel and

u-channel gluon diagrams among Figs.3.6 contribute to the DLA and t-channel gluon diagram does not give the DL term. This fact will be understood from the previous calculation in the case of QED, since these diagrams are same as Fig.3.3. The amplitude including both Fig.3.6a and Fig.3.6c is written down as,

$$M^p(s,\mu^2)|_{gluon} = \frac{-ig^2}{(2\pi)^4} 2 \int \frac{s^2 d\alpha d\beta d^2k_T}{2(s\alpha\beta + k_T^2 + i\varepsilon)(s\alpha(1+\beta) + k_T^2 + i\varepsilon)} M^p(s, |k_T^2|) \times \left[\frac{\hat{m}_s}{-s(\alpha-1)\beta + k_T^2 + i\varepsilon} + \frac{\hat{m}_u}{-s(\alpha+1)\beta + k_T^2 + i\varepsilon} \right]$$

Again, we obtain the soft gluon contributions by substituting the Sommerfeld-Watson expressions for M and by performing the integrations. The answer depends on the signature of the partial wave. The soft gluon contribution to the positive signature partial wave is given by

$$f^+(N)|_{gluon} = \frac{g^2}{8\pi^2} \frac{1}{N} \frac{d}{dN} ((\hat{m}_s - \hat{m}_u) f^+(N)). \tag{3.46}$$

And we obtain for the negative signature partial wave:

$$f^-(N)|_{gluon} = \frac{g^2}{8\pi^2} \frac{1}{N^2} \frac{d}{dN} (N(\hat{m}_s - \hat{m}_u) f^-(N)) - \frac{g^2}{8\pi^2} \frac{1}{N^2} (\hat{m}_s + \hat{m}_u) f^+(N). \tag{3.47}$$

Now, we can obtain the DLA expression for the quark-quark forward scattering amplitude. The equation for the DL amplitude is given by Fig.3.7.

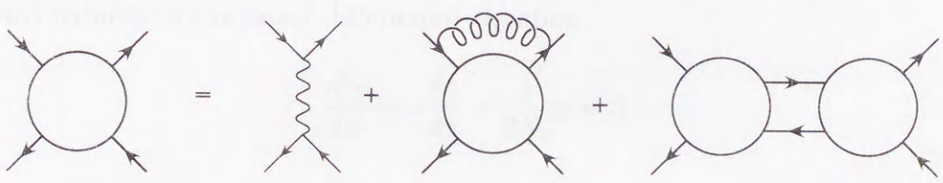

Figure 3.7:

Using the results for the soft quark and gluon contribution Eqs.(3.45,3.46,3.47), we are able to write down the equation giving DLA in terms of $f_i^p(N)$. The positive signature

amplitude leads to

$$f_i^+(N) = \frac{a_i g^2}{N} + \frac{b_i g^2}{8\pi^2}\frac{1}{N}\frac{d}{dN} f_i^+(N) + \frac{1}{8\pi^2}\frac{1}{N}(f_i^+(N))^2 \tag{3.48}$$

The coefficients are given by

$$a_0 = \frac{N_c^2 - 1}{2N_c}, \quad a_V = -\frac{1}{2N_c}, \quad b_0 = 0, \quad b_V = N_c, \quad c_0 = 0, \quad c_V = 1$$

The equations for the color singlet negative signature amplitudes are ,

$$f_0^-(N) = \frac{a_0 g^2}{N} - \frac{N_c^2 - 1}{N_c}\frac{g^2}{4\pi^2}\frac{1}{N}(f_0^-(N))^2 + \frac{1}{8\pi^2}\frac{1}{N}(f_0^-(N))^2.$$

This equation is solved easily. We obtain the Mellin amplitude for the color singlet channel,

$$f_0^-(N) = 4\pi^2 N\left(1 - \sqrt{1 - \frac{g^2(N_c^2-1)}{4\pi^2 N_c N^2}\left(1 - \frac{1}{2\pi^2 N} f_V^+(N)\right)}\right),$$

where we choose the minus sign in the front of the square root from the requirement that, the solution has to match the Born approximaton for large N, since the $N \to \infty$ means $x \to 1$. The amplitude $f_V(N)$ is obtained by solving the Riccati type equation (3.48). Using the transformation,

$$f_V^+(N) = N_c g^2 \frac{\partial}{\partial N} ln u(N).$$

Eq.(3.48) reduces to the linear differential equation

$$\frac{d^2u}{dz^2} - z\frac{du}{dz} - \frac{1}{2N_c}u = 0$$

where

$$z = N/N_0, \quad N_0 = \sqrt{N_c g^2/8\pi^2}$$

This equation is solved by a parabolic cylinder function. As a result, f_V^+ has the form:

$$f_V^{(+)}(N) = N_c g^2 \frac{d}{dN} ln(e^{z^2/4} D_{-1/2N_c^2}(z)) \tag{3.49}$$

$D_p(z)$ is the parabolic cylinder function [25].

Finally, let us consider the DLA for the virtual photon - quark scattering amplitude $\hat{T}^{\mu\nu}$. The imaginary parts of this amplitude are related to the DIS process for a quark target. We can decompose $\hat{T}^{\mu\nu}$ into the same tensor structures with the hadronic tensor

$$\hat{T}^{\mu\nu} = \hat{T}_S^{\mu\nu} + i\hat{T}_A^{\mu\nu}$$

with,

$$\begin{aligned}
\hat{T}_S^{\mu\nu} &= -\left(g_{\mu\nu} - \frac{q_\mu q_\nu}{q^2}\right)\hat{T}_1 + \left(p_\mu - \frac{p\cdot q}{q^2}q_\mu\right)\left(p_\nu - \frac{p\cdot q}{q^2}q_\nu\right)\frac{2\hat{T}_2}{p\cdot q}\,, \\
\hat{T}_A^{\mu\nu} &= 2m\varepsilon_{\mu\nu\lambda\sigma}q^\lambda\left\{s^\sigma\frac{\hat{T}_3}{p\cdot q} + (p\cdot q s^\sigma - q\cdot s p^\sigma)\frac{\hat{T}_4}{(p\cdot q)^2}\right\}\,.
\end{aligned}$$

The structure function for the quark target g_1^{quark} is obtained from $\hat{T}_3$ as,

$$g_1^{quark} = \frac{1}{\pi}Im\hat{T}_3$$

Notice that the amplitude $\hat{T}_3$ is anti-symmetric with respect to the replacement $s \to -s$. Indeed, the tensor $\hat{T}^{\mu\nu}$ is symmetric under the interchange of μ and ν and $q \to -q$. But $q \to -q$ means $x \to -x$, i.e. $s \to -s$. Since the tensors in the front of $\hat{T}_3$ is anti-symmetric, $\hat{T}_3$ must be anti-symmetric. Accordingly, $\hat{T}_3$ belongs to the negative signature amplitude. In the following, we shall concentrate on this negative signature amplitude $\hat{T}_3$ which gives g_1^{quark}. If $Q^2 \simeq \mu^2$, namely, the external photons are nearly on the mass-shell, the DLA equation for the photon-quark scattering is given by Fig.3.8.

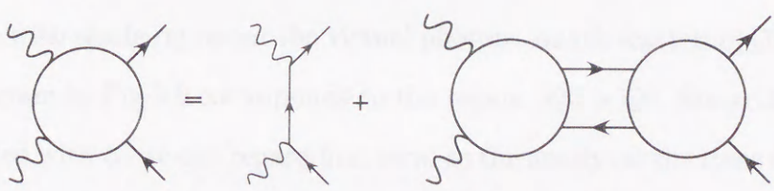

Figure 3.8:

The each blob represents the on-mass shell amplitude. Here, we introduce the Sommerfeld-Watson transformation for the photon-quark scattering in the same way as Eq.(3.44),

$$\hat{T}_3(s,\mu^2) = \int_{\delta-i\infty}^{\delta+i\infty} \frac{dN}{2\pi i} \left(\frac{s}{\mu^2}\right)^N \xi^{(-)} R_3(N) \tag{3.50}$$

The expression in terms of the partial waves R for the second diagram is obtained immediately by replacing f by R in Eq.(3.45). The DLA equation becomes

$$R_3(N) = \frac{c_3}{N} + \frac{1}{8\pi^2 N} f_0^- R_3(N),$$

where c_3 is $2e_i^2$.

The trivial solution of this equation is ,

$$R_3(N) = \frac{c_1}{N - f_0^-(N)/(8\pi^2)}.$$

At small x in the deep inelastic scattering which means $S \gg Q^2 \gg \mu^2$, the virtuality Q^2 of photon is not so small. Then we must divide the virtual photon quark scattering amplitude into two parts corresponding to the integration regions $|k_T^2| < Q^2$ and $|k_T^2| > Q^2$ (Fig.3.9).

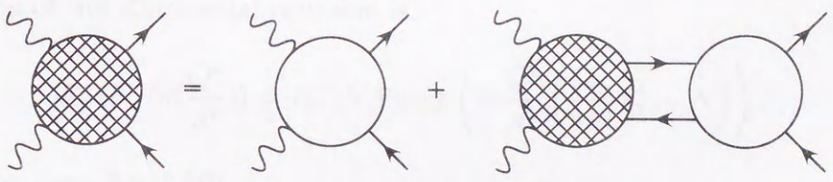

Figure 3.9:

The blobs with shade represent the virtual photon - quark scattering DL amplitude. The first diagram in Fig.3.9 corresponds to the region $|k_T^2| > Q^2$. Since the Q^2 is very small compared with S, we can regard first term as the nearly on the mass shell photon-quark scattering amplitude which we have already obtained. The second diagram is the soft quark contribution. Then, we get the following equation for Fig.3.9.

$$\hat{T}_3(s,\mu^2) = \hat{T}_3(s,Q^2) + \frac{-i}{(2\pi)^4}\int \frac{s^2 d\alpha d\beta d^2k_T(-2k_T^2)}{2(k_T^2+\alpha\beta s+i\varepsilon)^2}\frac{\hat{T}_{3i}(s\alpha,|k_T^2|)}{s\alpha+i\varepsilon}\frac{\hat{T}_{3i}(-s\beta,|k_T^2|)}{-s\beta+i\varepsilon}$$

Transforming into the Sommerfeld-Watson representation,

$$\int \frac{dN}{2\pi i}\left(\frac{s}{\mu^2}\right)^N R_3^-(N, ln\frac{Q^2}{\mu^2})$$
$$= \int \frac{dN}{2\pi i}\left(\frac{s}{Q^2}\right)^N R_3^-(N,0) + \int \frac{dN}{2\pi i}\frac{1}{8\pi^2}\int_{\mu^2}^{Q^2}\frac{d|k_T^2|}{|k_T^2|}\left(\frac{s}{k_T^2}\right)^N R_3^-(N, ln(\frac{Q^2}{k_T^2}))f_0^-(N)$$

and by factoring out $\int \frac{N}{2\pi i}(s/Q^2)^N$ from the both side, we have

$$\left(\frac{Q^2}{\mu^2}\right)^N R_3^-(N, ln\frac{Q^2}{\mu^2})$$
$$= R_3^-(N,0) + \frac{1}{8\pi^2}\int_{\mu^2}^{Q^2}\frac{d|k_T^2|}{|k_T^2|}\left(\frac{Q^2}{k_T^2}\right)^N R(N, ln(\frac{Q^2}{k_T^2}))f_0^-(N) \qquad (3.51)$$

This equation is solved easily by differentiating with respect to μ^2. Indeed, from Eq.(3.51), we obtain,

$$\mu^2\frac{d}{d\mu^2}R_3^-(N, ln(\frac{Q^2}{\mu^2})) = (\omega - \frac{1}{8\pi^2})f_0^-(\omega)R_3^-.$$

The solution of this differential equation is,

$$R_3^-(N, ln(\frac{Q^2}{\mu^2})) = R_3^-(N,0)exp\left(ln\frac{Q^2}{\mu^2}\left(\frac{1}{8\pi^2}f_0^- - N\right)\right).$$

Then, we get from Eq.(3.50)

$$\hat{T}_3 = 2e_i^2\int_{\delta-i\varepsilon}^{\delta+i\varepsilon}\frac{dN}{2\pi i}\left(\frac{s}{Q^2}\right)^N \xi^- \frac{1}{N - f_0^-(N)/8\pi^2}e^{ln\frac{Q^2}{\mu^2}f_0^-(N)/(8\pi^2)}.$$

In order to obtain a final result, g_1^{quark}, we have to take the discontinuity in s. With the signature factor $\xi^- = i\pi N/2$ and the variables $x \sim Q^2/s$ and Q^2 we arrive at

$$g_1^{quark}(x,Q^2) = \frac{e_i^2}{2}\int_{\delta-i\varepsilon}^{\delta+i\varepsilon}\frac{dN}{2\pi i}x^N\left(\frac{Q^2}{\mu^2}\right)^{f_0^-(N)/(8\pi^2)}\frac{N}{N - f_0^-(N)/8\pi^2}. \qquad (3.52)$$

In the next section , we discuss the physical implication of this DLA formula for g_1^{quark}.

3.3 The expansion of DLA formula

The solution of Eq.(3.4) with the fixed coupling α_s becomes

$$\Delta q(Q^2, N) = \Delta q(\mu^2, N) \left(\frac{Q^2}{\mu^2}\right)^{\gamma(\alpha_s, N)} \tag{3.53}$$

where we identify $Q_0^2 = \mu^2$. Since the initial parton density $\Delta q(\mu^2, N)$ in the case of the quark target is one, we obtain the moment space expression Eq.(3.3) for the parton as follows;

$$g_1^{quark}(Q^2, N) = \frac{e_i^2}{2} C(\alpha_s, N) \left(\frac{Q^2}{\mu^2}\right)^{\gamma(\alpha_s, N)} \tag{3.54}$$

In comparison with Eq.(3.52), we can identify the resummed anomalous dimension $\hat{\gamma}$ and the coefficient function $\hat{C}$ to be,

$$\hat{\gamma}(\alpha_s, N) \equiv \lim_{N\to 0} \gamma(\alpha_s, N) = -f_0^-(N)/8\pi^2 \,, \tag{3.55}$$

$$\hat{C}(\alpha_s, N) \equiv \lim_{N\to 0} C(\alpha_s, N) = \frac{N}{N - f_0^{(-)}(N)/8\pi^2} \,. \tag{3.56}$$

Now it will be instructive to re-expand Eqs.(3.55,3.56) in terms of α_s to see whether these formulae sum up the most singular terms of the perturbative series. The expressions expanded up to $\mathcal{O}(\alpha_s^5)$ read,

$$\begin{aligned}
\hat{\gamma} &= -N\left[2C_F\left(\frac{\bar{\alpha}_s}{N^2}\right) + 4C_F\left(C_F + \frac{2}{N_c}\right)\left(\frac{\bar{\alpha}_s}{N^2}\right)^2\right. \\
&\quad + 16C_F\left(C_F^2 + 2\frac{C_F}{N_c} - \frac{1}{2N_c^2} - 1\right)\left(\frac{\bar{\alpha}_s}{N^2}\right)^3 \\
&\quad \left. + 16C_F\left(5C_F^3 + 12\frac{C_F^2}{N_c} + 2\frac{C_F}{N_c^2} - 4C_F + \frac{1}{N_c^3} + \frac{5}{N_c} + 6N_c\right)\left(\frac{\bar{\alpha}_s}{N^2}\right)^4\right] \\
&\quad + \cdots \\
&= N\sum_{k=1}^{\infty} \hat{\gamma}^k \left(\frac{\bar{\alpha}_s}{N^2}\right)^k \,, \qquad (3.57) \\
\hat{C} &= 1 + 2C_F\left(\frac{\bar{\alpha}_s}{N^2}\right) + 8C_F\left(C_F + \frac{1}{N_c}\right)\left(\frac{\bar{\alpha}_s}{N^2}\right)^2 \\
&\quad + 8C_F\left(5C_F^2 + 8\frac{C_F}{N_c} - \frac{1}{N_c^2} - 2\right)\left(\frac{\bar{\alpha}_s}{N^2}\right)^3
\end{aligned}$$

$$+32C_F\left(7C_F^3+15\frac{C_F^2}{N_c}+2\frac{C_F}{N_c^2}-4C_F+\frac{1}{2N_c^3}+\frac{5}{2}\frac{1}{N_c}+3N_c\right)\left(\frac{\bar{\alpha}_s}{N^2}\right)^4$$
$$+\cdots$$
$$=\sum_{k=0}^{\infty}\hat{c}^k\left(\frac{\bar{\alpha}_s}{N^2}\right)^k . \tag{3.58}$$

These results coincide with the previous expectation of Eq.(3.6). Furthermore, noting the relation,

$$2C_A-3C_F=\frac{2}{N_c}+C_F ,$$

which holds in SU(N_c), we can see that the resummed expressions Eqs.(3.55,3.56) reproduce the known NLO results Eqs.(3.5) in the $\overline{\rm MS}$ scheme. Therefore, it is quite plausible that Eqs.(3.55,3.56) correctly sum up the "leading" singularities to all orders.

Here a comment is in order concerning the scheme dependence. It is well-known that the anomalous dimension and the coefficient function individually depend on the factorization scheme and only an appropriate combination of them becomes scheme independent. When one considers the higher order corrections in the perturbation theory, therefore, one must specify the scheme adopted. This means that we must be careful when considering the resummed quantities. In particular, the resummed "coefficient function" does not have any physical meaning until the scheme dependent part of the anomalous dimension is calculated in the same scheme. To clarify this issue, it is convenient to write the above results in the form which corresponds to the so-called DIS scheme [26]. The DIS scheme is defined so that the naive parton model relation is true to all orders in perturbation theory. The polarized parton densities become physical observable in this scheme. The parton densities and anomalous dimension in the DIS scheme are obtained by making the transformations,

$$\Delta q\to\Delta q^{DIS}\equiv C\Delta q ,$$
$$\gamma^{DIS}\equiv C\gamma C^{-1}-\beta(\alpha_s)\frac{\partial}{\partial\alpha_s}\ln C .$$

	LL	NLL	NNLL	$\cdots$
$o(\alpha)$	$\frac{1}{N}$			
$o(\alpha^2)$	$\frac{1}{N^3}$	$\frac{1}{N^2}$	$\frac{1}{N}$	
$o(\alpha^3)$	$\frac{1}{N^5}$	$\frac{1}{N^4}$	$\frac{1}{N^3}$	$\cdots$
$\vdots$	$\vdots$	$\vdots$	$\vdots$	$\vdots$
$o(\alpha^k)$	$N\frac{1}{N^{2k}}$	$N^2\frac{1}{N^{2k}}$	$N^3\frac{1}{N^k}$	$\cdots$
$\vdots$	$\vdots$	$\vdots$	$\vdots$	$\vdots$

Table 3.1:

Using the resummed $\hat{\gamma}$ and $\hat{C}$ Eqs.(3.57,3.58), we get the resummed part of the anomalous dimension in the DIS scheme,

$$\hat{\gamma}^{DIS} = N\sum_{k=1}^{\infty}\hat{\gamma}^k\left(\frac{\bar{\alpha}_s}{N^2}\right)^k + \beta_0 N^2\sum_{k=2}^{\infty}\hat{d}^k\left(\frac{\bar{\alpha}_s}{N^2}\right)^k + \mathcal{O}\left(N^3\left(\frac{\bar{\alpha}_s}{N^2}\right)^k\right), \tag{3.59}$$

where the second terms come from the resummed coefficient function and $\hat{d}^k$ are numerical numbers independent of N. The above equation tells us that the resummed coefficient function belongs to the NLL order corrections in the context of the resummation approach (see,Table[3.1]). The scheme dependence should be cancel among the terms which have the same singularity in each power of α_s. This fact implies that the LL resummed anomalous dimension $\hat{\gamma}$ being scheme independent and the analysis including only this part leads to a theoretically consistent result. This is the reason why the authors in Ref. [15] throw away the coefficient function. On the other hand, one must include the NLL order anomalous dimension which has not yet been available to see the effects of the coefficient function. To calculate the NLL order anomalous dimension, one must establish a factorization theorem explicitly. In the method to resum the double logarithmic corrections to all orders explained in section 3.2. the factorization of the mass singularities is unfortunately quite obscure since both the

mass and infra-red singularities are regularized by a common scale μ^2. Therefore it is impossible to calculate the NLL order anomalous dimension in the method of section 3.2. In fact, it has been pointed out by several people that the resummed results Eqs.(3.57,3.58) do not correspond to results in any known scheme beyond the NLO. It is very important and urgent to establish an appropriate factorization theorem á la "*High-Energy Factorization Theorem*"[34] for the unpolarized structure functions.

Chapter 4

Numerical analysis

Numerical analysis of the spin structure function g_1^{NS} in the small x region was done in the context of the small x resummation approach in Ref. [15]. They obtained the result that the small x resummation effect is not significant despite of a naive expectation discussed in Ref. [14]. In this chapter, we numerically reanalyze the behavior of g_1^{NS} structure function to show how the final results are sensitive to the choice of the input parton densities. In conjunction with the claim in Ref. [14], we also consider the effects from the resummed coefficient function. As already discussed in chapter 3, we can not include the coefficient function in a theoretically consistent way. However we believe that the inclusion of the coefficient function could shed some light on the size of the NLL corrections in the resummation approach. [28]

4.1 The numerical Mellin inversion technique

In this section, we explain our method to estimate the g_1^{NS} structure function numerically. Our starting point is the expression,

$$g_1^{NS}(Q^2,x) = \int_{c-i\infty}^{c+i\infty} \frac{dN}{2\pi i} x^{-N} \exp\left(-\int_{\alpha_s(Q_0^2)}^{\alpha_s(Q^2)} \frac{d\alpha_s}{\beta}\gamma^{DIS}\right) g_1^{NS}(Q_0^2,N)\ . \tag{4.1}$$

The anomalous dimension γ^{DIS} which includes the resummation of $\ln^n x$ terms is organized as follows,

$$\gamma^{DIS}(N) = \bar{\alpha}_s \gamma^1(N) + \bar{\alpha}_s^2 \gamma^2(N) + K(N, \alpha_s) - \beta \frac{\partial}{\partial \alpha_s} \ln\left(1 + \bar{\alpha}_s c^1 + H(N, \alpha_s)\right) \ , \quad (4.2)$$

where $\gamma^{1,2}$ and c^1 are respectively the usual anomalous dimension and coefficient function at the one and two-loop fixed order perturbation theory. $K(N, \alpha_s)$ $(H(N, \alpha_s))$ is the resummed anomalous dimension Eq.(3.57) (Eq.(3.58)) with $k = 1, 2$ $(k = 0, 1)$ terms being subtracted because those terms have already been included in the usual anomalous dimension and coefficient function.

$$\begin{aligned} K(N, \alpha_s) &\equiv \hat{\gamma}(N) - \hat{\gamma}^1 \frac{\bar{\alpha}_s}{N} - \hat{\gamma}^2 \frac{\bar{\alpha}_s^2}{N^3} \ , \\ H(N, \alpha_s) &\equiv \hat{C}(N) - 1 - \hat{c}^1 \frac{\bar{\alpha}_s}{N^2} \ . \end{aligned}$$

It should be noted here that the anomalous dimension at $N = 1$ plays a special role for the non-singlet g_1 structure function. In a language of the operator product expansion, $\gamma(N = 1)$ is the anomalous dimension of the (non-singlet) axial vector current. Since the (non-singlet) axial vector current is conserved, the corresponding anomalous dimension should vanish. The perturbation theory guarantees this symmetry order by order in the α_s expansion. However, the resummation of the leading singularities in N does not respect this symmetry. Therefore, we need to restore this symmetry "by hand". In this paper, we multiply $K(N, \alpha_s)$ by $(1 - N)$ [29],

$$K(N, \alpha_s) \to K(N, \alpha_s)(1 - N) \ .$$

which satisfies the condition of $\lim_{N \to 1} K(N, \alpha_s) = 0$. Of course, this is not a unique prescription and one can choose other procedure ,e.g,

$$K(N, \alpha_s) \to K(N, \alpha_s) - K(1, \alpha_s).$$

This procedure also fulfills the above condition. Although we have tried the analysis with this procedure, our final conclusion remains the same qualitatively.

Now let us explain how to perform the Mellin inversion Eq.(4.1) which is the integral in the complex N-plane. At first, we must know the Mellin transform of the input function $g_1(Q_0^2, N)$. It is easy to obtain an analytic form for it in the complex N-plane since we assume a simple function (see below) for the input density. Next we need an analytically continued expression of the anomalous dimension γ^{DIS} in the complex N-plane. For the g_1 structure function, only odd moments are defined. So we replace $(-1)^N$ by (-1) in the expression of the anomalous dimension obtained in Ref. [19]. The integration contour in the Mellin inversion should be on the right of the rightmost singularity of the integrand. The contour of the integration in Eq.(4.1) is displayed in Fig.(4.1) and denoted by C_0. The contour integration along the imaginary axis from $c-i\infty$ to $c+i\infty$ is numerically inconvenient due to the slow convergence of the integral in the large $|N|$ region.

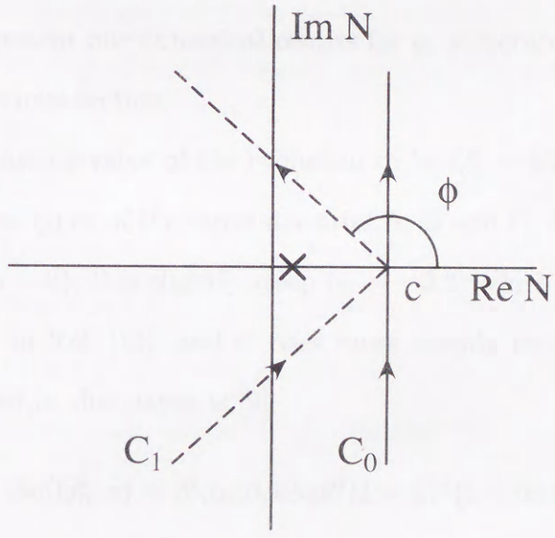

Figure 4.1:

To get rid of this problem, we deformed the contour to the line which have an angle ϕ ($\phi > \pi/2$) from the real N axis. The integration along this deformed contour C_1,

yields the same result as the original one as long as no singularities of $g_1(Q^2, N)$ are enclosed by $C_0 - C_1$. By using a relation $g_1^*(Q^2, N) = g_1(Q^2, N^*)$ ('$*$' denotes the complex conjugation), Eq.(4.1) can be written, for the contour characterized by c and ϕ in Fig.4.1

$$g_1^{NS}(Q^2, x) = \frac{1}{\pi}\int_0^\infty dz Im\left[exp(i\phi)x^{-c-zexp(i\phi)}g_1^{NS}(N = c + zexp(i\phi))\right].$$

By this change of the contour, we have a damping factor $\exp(ln(1/x)z\cos\phi)$ which strongly suppresses the contribution from the large $|N|$ region . In the integration along this new contour, we will be able to cut the large $|N|$ region, namely $0 \leq z \leq z_{max}$. Finally we have checked the stability of results by changing the contour parameter z_{max}, c, ϕ. One can find the details of this technique in Ref. [30].

4.2 The small x behavior of g_1 structure function

In this section, we present our numerical results for g_1 structure function by using the technique of the previous section.

We choose the starting value of the evolution to be $Q_0^2 = 4GeV^2$. We calculate the Q^2 evolution for three types of the input densities A, B and C: A is a function which is flat at small x ($x^\alpha, \alpha \sim 0$), B is slightly steep ($\alpha \sim -0.2$) which is essentially the same as one ($\alpha \sim -0.17$) in Ref. [15], and C rises more steeply ($\alpha \sim -0.7$). The explicit parameterization used in this paper is [9],

$$\Delta q(Q_0^2, x) = N(\alpha, \beta, a)\eta x^\alpha(1-x)^\beta(1+ax) \ ,$$

where N is a normalization factor such that $\int dx N x^\alpha(1-x)^\beta(1+ax) = 1$ and $\eta = \frac{1}{6}g_A/g_V$ ($g_A/g_V = 1.26$) in accordance with the Bjorken sum rule. A, B and C correspond to the following values of parameters,

$$A \ : \ \alpha = +0.0 \ , \ \beta = 3.09 \ , \ a = 2.23 \ ,$$

$$B \ : \ \alpha = -0.2 \ , \ \beta = 3.15 \ , \ a = 2.72 \ ,$$

$$C \ : \ \alpha = -0.5 \ , \ \beta = 2.41 \ , \ a = 0.02 \ .$$

In our analysis we put the flavor number $n_f = 4$ and $\Lambda_{QCD} = 0.23 GeV$.

First we estimate the case which includes only the LL correction $\hat{\gamma}$. The evolution kernel in this case is obtained by dropping $H(N, \alpha_s)$ in Eq.(4.2). This is a consistent approximation in the resummation approach. Fig.4.2a (4.2b,4.2c) shows the results (dashed curves) after evolving to $Q^2 = 10, 10^2, 10^4 GeV^2$ from the A (B, C) input density (dot-dashed line). The solid curves are the predictions of the NLO-DGLAP evolution. These results show a tiny enhancement compared with the NLO-DGLAP analysis and are consistent with those in Ref. [15]. In addition, we have also calculated g_1 with the same input function as one used by Blümlein and Vogt and could reproduce their results. In the case of C, we can not discriminate a difference between the LL and DGLAP results. The enhancement is, as expected, bigger when the input density is flatter. However any significant differences are not seen between the results from different input densities.

Next, we include the NLL corrections coming from the resummed "coefficient function". We show the results in Fig.4.3 by the dashed curves. (Other curves are the same as in Fig.4.2.) The results are rather surprising. The inclusion of the coefficient function leads to a strong suppression on the evolution of the structure function at small x. Since the effects from the coefficient function fall in the NLL level, the LL terms are expected to (should) dominate in the small x. However our results imply that the LL approximation is not sensible in the small x region we are interested in.

As the resummed coefficient function is only a part of the NLL correction, we can not present a definite conclusion on the (full) NLL correction. But it is obvious that the NLL correction is very important at the experimentally accessible region of x. In the following section, we explain why the coefficient function leads to such suppression.

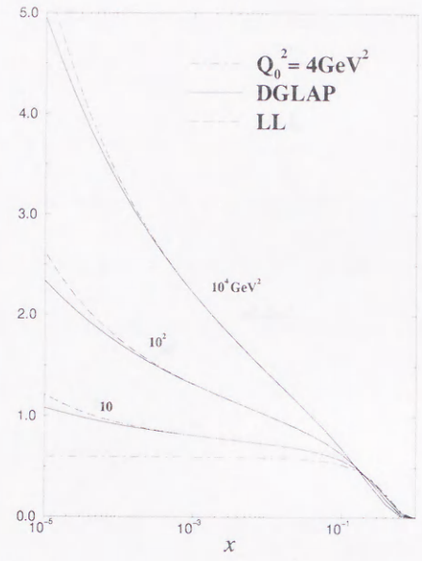

(a)

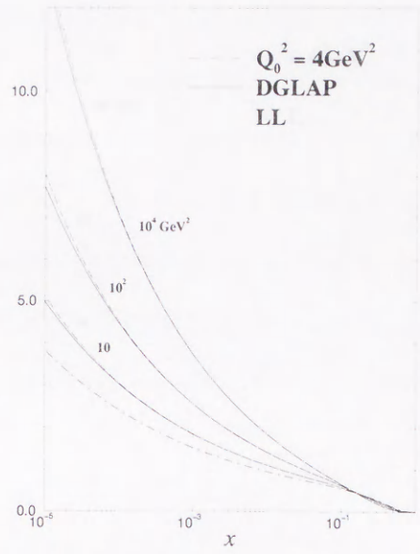

(b)

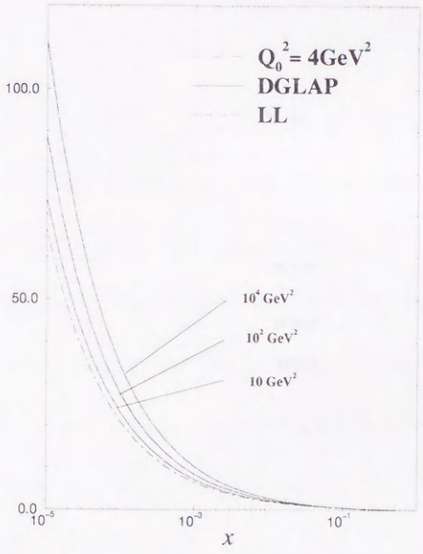

(c)

Figure 4.2: The LL evolution as compared to the DGLAP results with the flat input A (Fig. 4.2a) and steep ones B (Fig. 4.2b) and C (Fig. 4.2c).

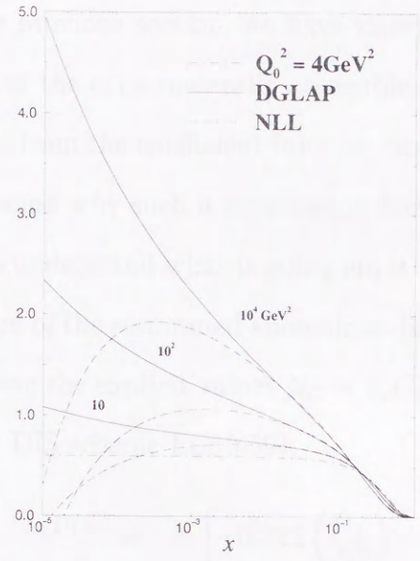

(a)

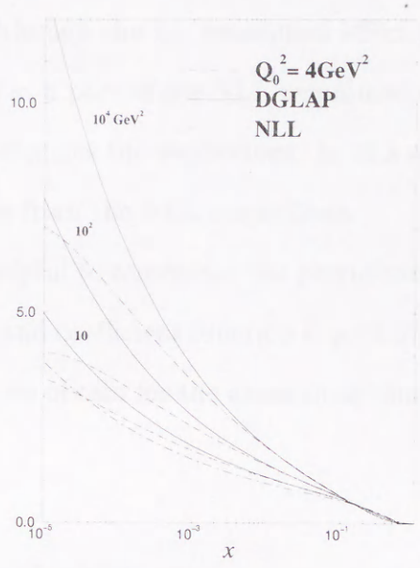

(b)

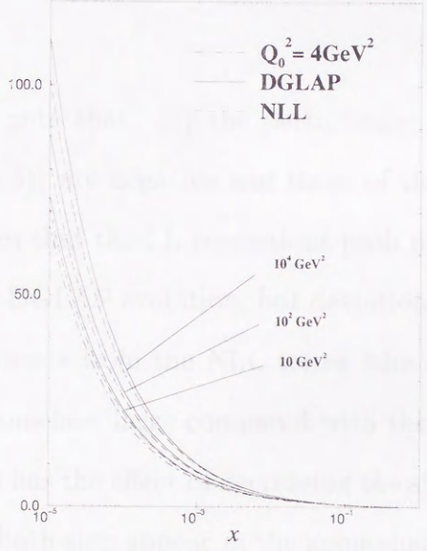

(c)

Figure 4.3: The NLL evolution as compared to the DGLAP results with the flat input A (Fig. 4.3a) and steep ones B (Fig. 4.3b) and C (Fig. 4.3c).

4.3 Discussion

In the previous section, we have shown that although the LL resummed effect is very small at the experimentally accessible region of x, a part of the NLL resummed contribution from the coefficient function drastically changes the predictions. In this section, we discuss why such a suppression factor comes from the NLL corrections.

To understand what is going on, it will be helpful to remember the perturbative expansion of the resummed anomalous dimension and coefficient function Eqs.(3.57,3.58). By using the explicit values $N_C = 3, C_F = 4/3$, we obtain for the anomalous dimension in the DIS scheme Eq.(3.59),

$$\begin{aligned}\hat{\gamma}^{DIS} &= N\left[-0.212\left(\frac{\alpha_s}{N^2}\right)\right. \\ &\qquad \left. - 0.068\left(\frac{\alpha_s}{N^2}\right)^2 - 0.017\left(\frac{\alpha_s}{N^2}\right)^3 - 0.029\left(\frac{\alpha_s}{N^2}\right)^4 + \cdots\right] \\ &+ N^2\left[0.141\left(\frac{\alpha_s}{N^2}\right)^2 + 0.119\left(\frac{\alpha_s}{N^2}\right)^3 + 0.069\left(\frac{\alpha_s}{N^2}\right)^4 + \cdots\right] \\ &+ \cdots .\end{aligned} \tag{4.3}$$

Here note that: (1) the perturbative coefficients of the LL terms (the first part of Eq.(4.3)) are negative and those of the higher orders are rather small number. This implies that the LL corrections push up the structure function compared to the fixed-order DGLAP evolution, but deviations are expected to be small. (2) the perturbative coefficients from the NLL terms (the second part of Eq.(4.3)), however, are positive and somehow large compared with those of the LL terms. This positivity of the NLL terms has the effect of decreasing the structure function. This fact that the coefficients with both sign appear in the anomalous dimension should be contrasted with the case of the unpolarized structure function [31].

Now it might be also helpful to *assume* that the saddle-point dominates the Mellin inversion Eq.(4.1). We have numerically estimated the approximate position of the

saddle-point and found that the saddle-point stays around $N_{SP} \sim 0.31$ in the region of $x \sim 10^{-5}$ to 10^{-2}. (Of course the precise value of the saddle-point depends on x, Q_0^2 and Q^2.) By looking at the explicit values of the coefficients in Eq.(4.3), the position of the saddle-point seems to suggest that the NLL terms can not be neglected. Since the coefficients from the higher order terms are not so large numerically, it is also expected that the terms which lead to sizable effects on the evolution may be only first few terms in the perturbative series in the region of x we are interested in. We have checked that the inclusion of the first few terms in Eq.(4.3) already reproduces the results of section 4.2.

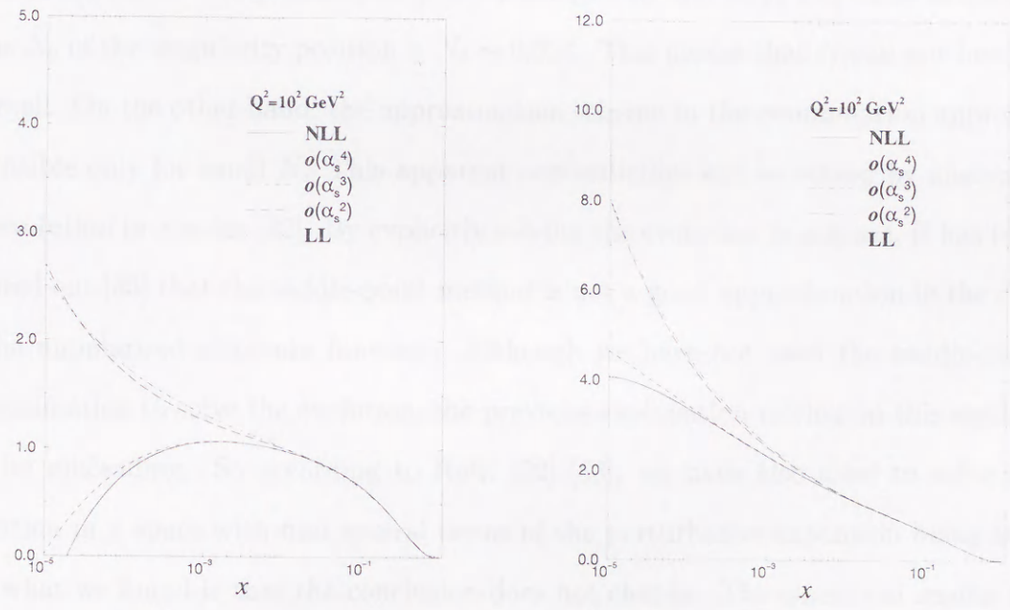

(a) (b)

Figure 4.4: Contributions from the fixed order terms in the NLL resummation with the flat input A (Fig. 4.4a) and steep one B (Fig. 4.4b).

Fig.4.4a (4.4b) shows the numerical results of the contribution from each terms of

the NLL corrections in Eq.(4.3) at $Q^2 = 10^2 GeV^2$ with the A (B) type input density. The solid (dot-dashed) line corresponds to the NLL (LL) result. The long-dashed, dashed and dotted lines correspond respectively to the case in which the terms up to the order α_s^2, α_s^3, α_s^4, are kept in the NLL contributions. One can see that the dotted line already coincides with the full NLL (solid) line. These considerations could help us to understand why the NLL corrections turns out to give large effects on the evolution of the g_1 structure function.

The final discussion concerns the convergence issue of the perturbative series. As discussed in Refs. [32] [33], one must be careful when applying the perturbative approach to the small x evolution. The integrand in Eq.(4.1) has a singularity in the moment space. This (rightmost) singularity is equal to that of $f_0^-(N)$. The numerical value N_0 of the singularity position is $N_0 \sim 0.304$. This means that N can not become so small. On the other hand, the approximation scheme in the resummation approach is sensible only for small N. This apparent contradiction will be solved by analyzing the evolution in x space [32]. By explicitly solving the evolution in x space, it has been pointed out [33] that the saddle-point method is not a good approximation in the case of the unpolarized structure function. Although we have not used the saddle-point approximation to solve the evolution, the previous explanation relying on this method can be misleading. So according to Refs. [32] [33], we have also tried to solve the evolution in x space with first several terms of the perturbative expansion being kept and what we found is that the conclusion does not change. The numerical results are essentially the same as Fig.4.4.

Chapter 5

Summary

We have numerically studied the small x behavior of the flavor non-singlet $g_1(x, Q^2)$ structure function by taking into account the resummed effects of $\alpha_s ln^2 x$. After giving a basic kinematics of the process we are interested in, in chapter 3 we gave a brief review of the resummation procedure of $\alpha_s ln^2 x$ terms firstly developed by Kirschner and Lipatov [13], and gave the resummed expression for the partonic structure function g_1^{parton}. We extracted the resummed anomalous dimension and coefficient function from this resummed partonic structure function. By expanding this expression in terms of α_s, we verified the resummed result reproduces the known corrections up to $o(\alpha_s^2)$. We pointed out that the resummed coefficient function belongs to the NLL corrections in the context of the resummation approach. In chapter 4, we explained the method of numerical Mellin-inversion in detail and showed our numerical results. Our analysis including only the LL terms supports the results by Blümlein and Vogt [15]. Namely, there is no significant contribution from the resummed terms even at $x \sim 10^{-5}$. We also studied the Q^2 evolution from various input densities, steep and flat and found that there is no significant difference between the results from different input densities. Next we have performed the analysis which includes the resummed coefficient function in the light of the assertion of Bartels, Ermolaev and Ryskin [14], though this is not theoretically consistent as pointed out in chapter 3. Our results suggest that the LL

approximation is unstable in the sense that a large suppression effect comes from the resummed coefficient function which should be the NLL correction. In the final section of chapter 4, we have discussed why the inclusion of a part of the NLL corrections leads to such unexpected results.

Finally, the future polarized HERA experiment will provide us with many data on g_1 at small x. However, the theoretical study which takes into account the small x resummation is still premature for the polarized structure function compared with the unpolarized structure function. As already pointed out in chapter 3, there is no factorization theorem concerning the lnx singularities for the polarized structure function which should correspond to the *High-energy factorization theorem* [34] for the unpolarized structure function. Since our results show that we need a full NLL analysis to make a definite prediction at small x, the establishment of an appropriate factorization theorem is an urgent subject in this field.

Acknowledgments

Main part of this thesis is based on the work in collaboration with Prof.J.Kodaira and Y.Kiyo. The author would like to thank his collaborators and Prof.M.Hirata, Prof.K.Tanaka for discussions. The author also would like to thank T.Nasuno, Dr.H-T.Sato and Dr.S.Kanemura for encouraging him. Thanks are also due to Prof.J.Kodaira for careful reading of the manuscript and many suggestions.

Appendix A

QCD Lagrangian and Feynman rules

The QCD Lagrangian is given by

$$\mathcal{L} = \overline{\psi}^i (i\gamma^\mu D_\mu^{ij} - m\delta^{ij}\psi^j) - \frac{1}{4} F_{\mu\nu}^a F^{a\mu\nu} - \frac{1}{2\alpha}(\partial^\mu A_\mu^a)^2 + (\partial^\mu \overline{\chi} D_\mu^{ab} \chi^b)$$

where, ψ is a quark field, A_μ^a is a gluon field and χ ($\overline{\chi}$) is a ghost (anti-ghost) field. $F_{\mu\nu}^a$ is the field strength tensor;

$$F_{\mu\nu}^a = \partial_\mu A_\nu^a - \partial_\nu A_\mu^a + g f^{abc} A_\mu^b A_\nu^c$$

The covariant derivative D_μ is, for the fundamental representation,

$$D_\mu^{ij} = \partial_\mu \delta^{ij} - ig A_\mu^a T^{aij}$$

and

$$D_\mu^{ab} = \partial_\mu \delta^{ab} - g f^{abc} A_\mu^c$$

for the adjoint representation. Feynman rules for QCD are given by follows,

- Propagators

  · quark

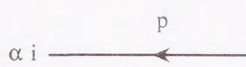

$$iS_F^{ij}(p)_{\alpha\beta} = \left(\frac{i\delta^{ij}}{\not{p} - m + i\varepsilon} \right)_{\alpha\beta}$$

· gluon

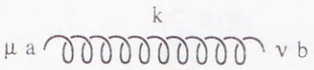

$$i\Delta^{ab}_{\mu\nu}(k) = \frac{-i\delta^{ab}}{k^2 + i\varepsilon}\left(g_{\mu\nu} - (1-\alpha)\frac{k_\mu k_\nu}{k^2}\right)$$

· ghost

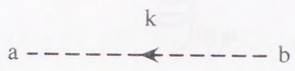

$$i\Delta^{ab}(k) = \frac{-i\delta^{ab}}{k^2 + i\varepsilon}$$

• Vertices

· quark-gluon vertex

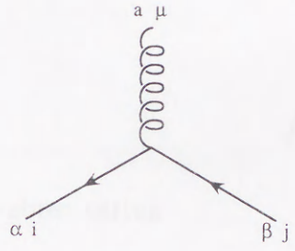

$$ig\gamma^{\mu}_{\alpha\beta}T^{a}_{ij}$$

· 3-gluon vertex

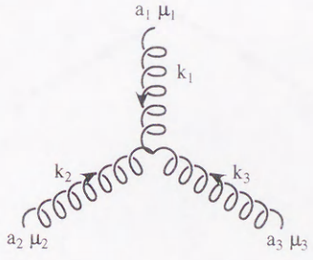

$$gf^{a_1a_2a_3}V_{\mu_1\mu_2\mu_3}(k_1,k_2,k_3)$$

where,

$$V_{\mu_1\mu_2\mu_3}(k_1,k_2,k_3) = (k_1-k_2)_{\mu_3}g_{\mu_1\mu_2} + (k_2-k_3)_{\mu_1}g_{\mu_2\mu_3} + (k_1-k_3)_{\mu_2}g_{\mu_3\mu_1}$$

· 4-gluon vertex

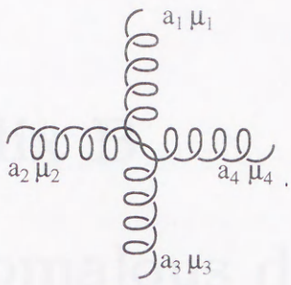

$$-ig^2 W^{a_1 a_2 a_3 a_4}_{\mu_1 \mu_2 \mu_3 \mu_4}$$

where,

$$\begin{aligned} & W^{a_1 a_2 a_3 a_4}_{\mu_1 \mu_2 \mu_3 \mu_4} \\ &= (f^{13,24} - f^{14,32}) g_{\mu_1 \mu_2} g_{\mu_3 \mu_4} + (f^{12,34} - f^{14,23}) g_{\mu_1 \mu_3} g_{\mu_2 \mu_4} \\ &+ (f^{13,42} - f^{12,34}) g_{\mu_1 \mu_4} g_{\mu_3 \mu_2} \end{aligned}$$

with

$$f^{ij,kl} = f^{a_i a_j a} f^{a_k a_l a}.$$

· gluon-ghost vertex

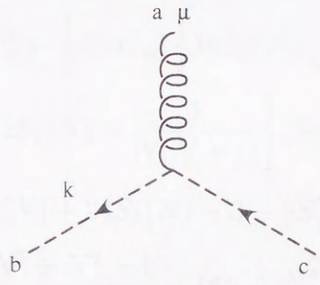

$$g f^{abc} k_\mu$$

Appendix B

The anomalous dimension and the coefficient function

We give the coefficients of the anomalous dimension, γ^1, γ^2 and the coefficient function c^1 for the flavor non-singlet part used in chapter 3,4 and introduce the useful formula given in Ref. [30]. The coefficients of the anomalous dimension are given by [19],

$$\gamma^1(N) = C_F(1 - \frac{2}{N(N+1)} + 4\sum_{j=2}^{N}\frac{1}{j}) \tag{B.1}$$

$$\begin{aligned}
\gamma^2(N) &= \frac{1}{2}(C_F^2 - \frac{1}{2}C_F C_A)\left\{16S_1(N)\frac{2N+1}{N^2(N+1)^2}\right. \\
&+ 16\left[2S_1(N) - \frac{1}{N(N+1)}\right][S_2(N) - S_2'(\frac{1}{2}N)] \\
&+ 64\tilde{S}(N) + 24S_2(N) - 3 - 8S_3'(\frac{1}{2}N) \\
&- \left. 8\,\frac{3N^3+N^2-1}{N^3(N+1)^3} - 16(-1)^N\frac{2N^2+2N+1}{N^3(N+1)^3}\right\} \\
&+ \frac{1}{2}C_F C_A\left\{S_1(N)\left[\frac{536}{9} + 8\frac{2N+1}{N^2(N+1)^2}\right] - 16S_1(N)S_2(N)\right. \\
&+ S_2(N)\left[-\frac{52}{3} + \frac{8}{N(N+1)}\right] - \frac{43}{6} - 4\frac{151N^4+263N^3+97N^2+3N+9}{9N^3(N+1)^3}\Big\} \\
&+ \frac{C_F n_F}{4}\left\{-\frac{160}{9}S_1(N) + \frac{32}{3}S_2(N) + \frac{4}{3} + 16\frac{11N^2+5N-3}{9N^2(N+1)^2}\right\}
\end{aligned} \tag{B.2}$$

For the coefficient function part, c^1 is given by [18]

$$c^1 = C_F\left(-9+\frac{1}{N}+\frac{2}{N+1}+\frac{2}{N^2}+3S_1(N)-4S_2(N)-\frac{2}{N(N+1)}S_1(N)+4G_1(N)\right). \tag{B.3}$$

Here, group factors for color $SU(N_c)$ are, $C_F = \frac{N_c^2-1}{2N_c}$ $C_A = N_c$ and n_f is the active flavor number. In above expressions, we defined the following sums,

$$S_l(N) = \sum_{j=1}^{N}\frac{1}{j^l}, \tag{B.4}$$

$$S_l'(\frac{1}{2}N) = \frac{1+(-1)^N}{2}S_l(\frac{1}{2}N)\frac{1-(-1)^N}{2}S_l(\frac{N-1}{2}), \tag{B.5}$$

$$\tilde{S}(N) = \sum_{j=1}^{N}\frac{(-1)^j}{j^2}S_1(j), \tag{B.6}$$

$$G_1(N) = \sum_{j=1}^{N}\frac{1}{j}\sum_{l=1}^{j}\frac{1}{l} \tag{B.7}$$

The analytic continuations of γ_1, γ_2, c^1in N, is required in order to perform the Mellin inversion numerically. The above non-trivial sums is continued in the following way,

$$S_1(N) = \gamma_E + \psi(N+1), \qquad \gamma_E = 0.577216 \tag{B.8}$$

$$S_2(N) = \zeta(2) - \psi'(N+1), \qquad \zeta(2) = \frac{\pi^2}{6} \tag{B.9}$$

$$S_3(N) = \zeta(3) + \frac{1}{2}\psi''(N+1), \qquad \zeta(3) = 1.202057 \tag{B.10}$$

$$G_1(N) = \frac{1}{2}\{S_1^2(N) + S_2(N)\} \tag{B.11}$$

where $\psi^{(n)} = d^{n+1}ln\Gamma(z)/dz^{n+1}$.

$$\begin{aligned}\tilde{S}(N) &= -\frac{5}{8}\zeta(3) \\ &+ (-1)^N\left[\frac{S_1(N)}{N^2} - \frac{\zeta(2)}{2}G(N) + \int_0^1 dx x^{N-1}\frac{Li_2(x)}{1+x}\right]\end{aligned} \tag{B.12}$$

with

$$G(N) \equiv \psi(N/2+1/2) - \psi(N/2). \tag{B.13}$$

$$Li_2(x) = -\int_0^x \frac{1}{z}ln(1-z)dz \tag{B.14}$$

Although the integral in Eq.(B.12) involving the Spence function $Li_2(x)$ cannot be reduced to a known analytic function anymore, the simple and sufficiently accurate expression was given as follows;

$$\frac{Li_2(x)}{1+x} \cong 1.010x - 0.846x^2 + 1.155x^3 - 1.074x^4 + 0.550x^5 \tag{B.15}$$

The various ψ functions and their derivatives appearing in the above expressions were calculated, for $Rez \geq 10$, with the help following asymptotic expansions

$$\psi(z) \cong lnz - \frac{1}{2z} - \frac{1}{12z^2} + \frac{1}{120z^4} - \frac{1}{256z^6} \tag{B.16}$$

$$\psi'(x) \cong \frac{1}{z} + \frac{1}{2z^2} + \frac{1}{6z^3} - \frac{1}{30z^5} + \frac{1}{42z^7} - \frac{1}{30z^9} \tag{B.17}$$

$$\psi''(z) \cong -\frac{1}{z^2} - \frac{1}{z^3} - \frac{1}{2z^4} + \frac{1}{6z^6} - \frac{1}{6z^8} + \frac{3}{10z^{10}} - \frac{5}{6z^{12}} \tag{B.18}$$

For $Rez < 10$ we have used the recursion relation

$$\psi^{(n)}(z+1) = \psi^{(n)}(z) + (-1)^n n! z^{-n-1} \tag{B.19}$$

in order to reach $\psi^{(n)}$ with $Rez \geq 10$.

Bibliography

[1] H.Böttcher,hep-ph/9712458.

[2] J.D.Bjorken,*Phys. Rev.***148** (1966) 1467;*ibid.* **D1** (1970) 1376.

[3] J.Ellis and R.L.Jaffe,*Phys. Rev.***D9** (1974) 1444;*ibid.* **D10** (1974) 1669.

[4] R. L. Heimann, *Nucl. Phys.* **B64** (1973) 429.

[5] J. Ashman *et al. Phys. Lett.* **B206** (1988) 364;
V. W. Hughes *et al. Phys. Lett.* **B212** (1988) 511;
B. Adeva *et al. Phys. Lett.* **B302** (1993) 553; **B320** (1994) 400;
D. Adams *et al., Phys. Lett.* **B329** (1994) 399; **B336** (1994) 125;
P. L. Anthony *et al. Phys. Rev. Lett.* **71** (1993) 959;
K. Abe *et al. Phys. Rev. Lett.* **74** (1995) 346; *ibid.* **75** (1995) 25; *ibid.* **76** (1996) 587.

[6] For a general review of QCD factorization see, for example, J. C. Collins, D. E. Soper and G. Sterman, in *Perturbative Quantum Chromodynamics*, edited by A. H. Mueller (World Scientific, Singapore, 1989).

[7] G. Altarelli, *Phys. Rep.* **81** (1982) 1 and references therein.

[8] G. Altarelli, R. D. Ball, S. Forte and G. Ridolfi *Nucl. Phys.* **B496** (1997) 337.

[9] R. D. Ball, S. Forte and G. Ridolfi, *Nucl. Phys.* **B444** (1995) 287; *Phys. Lett.* **B378** (1996) 255.

[10] M. Glück, E. Reya and W. Vogelsang, *Phys. Lett.* **B359** (1995) 201;
M. Glück, E. Reya, M. Stratmann and W. Vogelsang, *Phys. Rev.* **D53** (1996) 4775.

[11] V. V. Sudakov, *Sov. Phys. JETP* **3** (1956) 65.

[12] V. G. Gorshkov, V. N. Gribov, L. N. Lipatov, and G. V.Frolov, *Sov.J.Nucl.Phys.* **6** (1967) 95.

[13] R. Kirschner and L. N. Lipatov, *Nucl. Phys.* **B213** (1983) 122.

[14] J. Bartels, B. I. Ermolaev and M. G. Ryskin, *Z. Phys.* **C70** (1996) 273; *ibid.* **C72** (1997) 627.

[15] J. Blümlein and A. Vogt ,*Phys. Lett.* **B370** (1996) 149 ; *Acta.Phys.Polonica* **B27** (1996) 1309;
J. Blümlein, S. Riemersma and A. Vogt, hep-ph/9608470.

[16] EMC,J.Ashman *et al.*,*Phys. Lett.***B206** (1988) 364.; *Nucl. Phys.***B328** (1989) 1.

[17] S.A.Larin, F.V. Tkachev, and J.A.M. Vermaseren, *Phys. Rev. Lett.***66** (1991) 862;
S.A.Larin and J.A.M. Vermaseren, *Phys. Lett.***B259** (1991) 345.

[18] J. Kodaira, S. Matsuda, T. Muta, K. Sasaki and T. Uematsu, *Phys. Rev.* **D20** (1979) 627;
J. Kodaira, S. Matsuda, K. Sasaki and T. Uematsu, *Nucl. Phys.* **B159** (1979) 99.

[19] E. G. Floratos, D. A. Ross and C. T. Sachrajda, *Nucl. Phys.* **B129** (1977) 66; (E): **B139** (1978) 545; **B152** (1979) 493;
A. Gonzalez-Arroyo, C. Lopez and F. J. Yndurain, *Nucl. Phys.* **B153** (1979) 161;
A. Gonzalez-Arroyo and C. Lopez, *Nucl. Phys.* **B166** (1980) 429;
E. G. Floratos, C. Kounnas and R. Lacaze, *Nucl. Phys.* **B192** (1981) 417; *Phys. Lett.* **B98** (1981) 89;
G. Curci, W. Furmanski and R. Petronzio, *Nucl. Phys.* **B175** (1980) 27;
W. Furmanski and R. Petronzio, *Phys. Lett.* **B97** (1980) 437 ; *Z. Phys.* **C11** (1982) 293 ;
R. Mertig and W. L. van Neerven, *Z. Phys.* **C70** (1996) 637.

[20] B. I. Ermolaev, S. I. Manayenkov and M. G. Ryskin, *Z. Phys.* **C69** (1996) 259.

[21] L. N. Lipatov, *Sov. J. Nucl. Phys.* **23** (1976) 338;
E. A. Kuraev, L. N. Lipatov and V. S. Fadin, *Sov. Phys. JETP* **45** (1977) 199;
Ya. Balitskii and L. N. Lipatov, *Sov. J. Nucl. Phys.* **28** (1978) 822.

[22] Yu. L. Dokshizer, *Sov. Phys. JETP* **46**(1977) 641.

[23] V. N. Gribov and L. N. Lipatov, *Sov.J.Nucl.Phys.* **15** (1972) 438, 675.

[24] E. M. Lifshitz and L. P. Pitaevskiĭ, *Relativistic Quantum Theory* Section.13 (Pergamon Press Ltd,1974).

[25] I. S. Gradshtein and I. M. Ryzhik, *Table of Integrals, Series and Products* (**DVW, Berlin**) Section 9.24-9.25.

[26] G. Altarelli, R. K. Ellis and G. Martinelli, *Nucl. Phys.* **B157** (1979) 461.

[27] V. G. Gorshkov, L. N. Lipatov and M. M. Nesterov, *Yad.Fiz.* **9** (1969) 1221.

[28] Y. Kiyo, J. Kodaira and H. Tochimura, *Z.Phys.* **C74** (1997) 631;hep-ph/9711260.

[29] K. Ellis, F. Hautmann and B. Webber, *Phys. Lett.* **B348** (1995) 582.

[30] M. Glück, E. Reya and A. Vogt, *Z. Phys.* **C48** (1990) 471;
D. Graudenz, M. Hampel, A. Vogt and Ch. Berger, *Z. Phys.* **C70** (1996) 70.

[31] S. Catani, *Z. Phys.* **C70** (1996) 263.

[32] R. D. Ball and S. Forte, *Phys. Lett.* **B351** (1995) 313.

[33] J. R. Forshaw, R. G. Roberts and R. S. Thorne, *Phys. Lett.* **B356** (1995) 79.

[34] S. Catani and F. Hautmann, *Nucl. Phys.* **B427** (1994) 475 and references therein.

‡Reviews and text books for the perturbative QCD,

[35] J.Kodaira,*Prog. Theor. Phys. Suppl.***No.120**(1995) 37.

[36] T.Muta, *Foundations of Quantum Chromodynamics* (World Sientific,1987).

[37] G.Sterman et.al, *Handbook of perturbative QCD Rev. Mod. Phys.***67** (1995) 157.

[38] R.L.Jaffe,hep-ph/9602236.